DESIGN, BUILD, AND CONTROL OF A CLIMBING ROBOT FOR IRREGULAR SURFACE GEOMETRY

A Thesis

by

ALEXANDER JULIAN STOCKTON

Submitted to the Office of Graduate and Professional Studies of
Texas A&M University
in partial fulfillment of the requirements for the degree of

MASTER OF SCIENCE

Chair of Committee,	Sheng-Jen Hsieh
Committee Members,	Won-jong Kim
	Paul Cizmas
Head of Department,	Andreas Polycarpou

December 2015

Major Subject: Mechanical Engineering

ABSTRACT

Climbing robots are ideal for situations were maintenance and inspection tasks can cause people to be in dangerous situations or require them to be present for extended periods of time. Applications include inspection, testing, civil construction, cleaning, transport and security. The focus of this thesis was on robots that used pneumatic means to attain adhesion and wheels for locomotion. Research objectives include designing or utilizing a pneumatic based adhesion method to allow the robot to stick to concrete, brick, glass, or other such surfaces; climb on a surface with the lowest possible coefficient of friction between it and the robot; have the ability to overcome a step-like obstacle while climbing; use a single body to passively transition through sharp surface changes while climbing; have the ability to traverse over a gap-type obstacle while climbing without loss of adhesion or mobility.

To complete the objectives, a test rig was created that comprised of three surfaces that were hinged together and could be locked into place using aluminum struts at the hinge joint. Different material pallets were created and adhered to plywood that was then mounted to the test rig with screws. The robot was designed and built around laser cut and 3D printed parts.

From the experiments it was found that the robot could adhere to a glass surface with a coefficient of friction of 0.43 between it and the glass. Furthermore it was able to overcome a 15mm tall speedbump while climbing without loss of adhesion as well as being able to passively transition between surfaces that had an acute angle of 80° between them and do wall to ceiling transitions. Finally the robot was able to pass over a 55mm gap that was 23mm deep while climbing on a concrete surface.

It was concluded that by using thrust based adhesion the robot could handle a diverse array of surfaces and even gain greater ability to overcome obstacles while climbing. Future directions would improve on the robot by adding treads or multiple bodies to improve its base abilities.

TABLE OF CONTENTS

Page

LIST OF FIGURES

Page

LIST OF TABLES

Page

I INTRODUCTION

I A Motivation

Climbing robots are highly desirable in situations where it is quite dangerous for humans to be present or when the task at hand might require the person to be present for an extended period of time. These types of robots are ideal for maintenance and inspection tasks in industrial settings. Applications include inspection, testing, civil construction, cleaning, transport and security [1]. For these reasons climbing robots have been the subject of lots of research by universities such as London South Bank University, Institute of Engineering in Portugal, and the University of Pennsylvania as well as other companies such as Helical Robotics [2], [3], [4], [5].

Currently, the tasks listed above are completed by humans. Usually one or more workers are strapped into harnesses and then repel down or are hoisted up to the desired location. Once in place the worker can start their task but are limited by what they can carry. In some cases platforms are used when large equipment is needed but in all cases this is very difficult when the surface is curved at an inverted angle. In addition the workers are subject to the local weather conditions. The weather is a constant potential danger to workers and can lead to major delays for inspection and maintenance projects.

In order for robots to achieve climbing motion, proper adhesion to the climbing surface is necessary. This has been a difficult task in the past and is the subject of many researchers. Current methods of adhesion include suction, magnetic force, sharp talon hooks, compressive friction (in the case where the climbing surface is a pole), thrust force, and dry adhesion [1], [3], [4], [6], [7]. As for locomotion, most all choices either use wheels, tank style treads, or some number of legs to walk, [1], [8], [9]. Usually when it comes to circumnavigating obstacles, legged robots usually perform the best but at the cost of slower speeds, [7], [9], [10].

Because of their high versatility, the major goals of climbing robots are the ability to carry large payloads, high mobility, fast climbing speeds, dexterity in avoiding or overcoming obstacles, the ability to transition between surfaces, and the ability to climb multiple types of surfaces. Particularly, a group called Nine Sigma is interested in a robot that is able to climb up large concrete structures. Examples include dams and water silos for nuclear power facilities.

I B Nature of the Problem

Climbing robots are being increasingly study and developed for situations where it is difficult or undesirable for humans to be present. The problems that climbing robots must overcome can be placed into two basic categories. First is the robot's ability to adhere to surfaces that may have varying coefficients of friction. The second is its

ability to traverse over irregular or rough geometry. An optional issue in many cases, and an area for great improvement, is the robustness of a robot's abilities.

I B 1) Adhering to Surfaces

The task of climbing a multitude of different types of surfaces with unpredictable surface qualities is a challenging task for robots. While climbing, the robot is constantly battling gravity forces with frictional forces. To increase the frictional force, a large normal force is needed, or a naturally large coefficient of friction value between the robot and the surface. This is where the adhesion mechanism comes into play. In the case where the coefficient of friction between the robot and the surface is low, the adhesion mechanism must provide a large normal force in order to have a high frictional force. To accomplish this many robots use magnets, negative pneumatic pressure, or thrust.

Another approach is to simply have a naturally high coefficient of friction between the robot and many general materials. For this, dry fibular adhesive is usually used [11], [12], [13]. These consist of pads that have lots of micro scale fibers or mushroom-like heads [14]. The micro features are able to form a strong bond with a surface due to Van der Waal forces [11], [15], [14].

Below in Figure 1, a diagram of the robot at a general angle is shown and all the forces that act on it. From there, equations for the required thrust force as well as the coefficient of friction are generated.

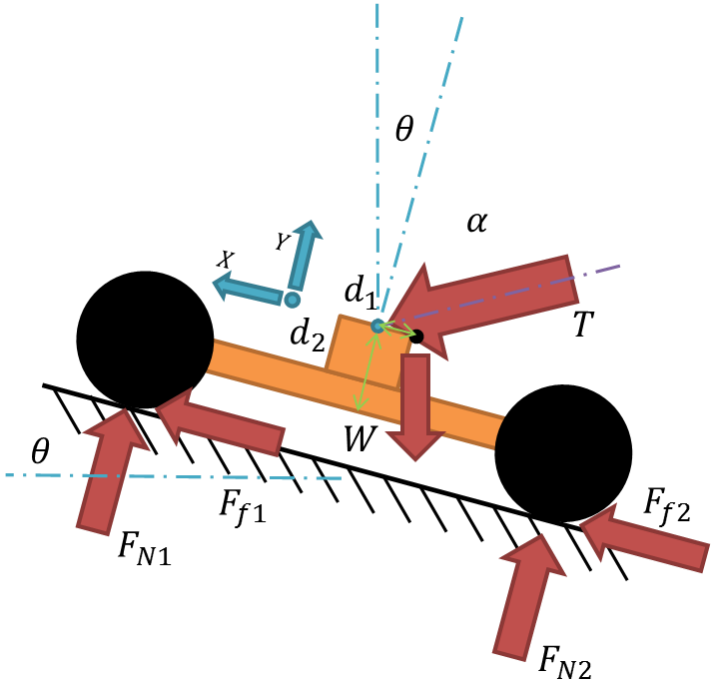

Figure 1: Free Body Diagram of a Climbing Robot

Forces can be broken down into x and y components and the thrust force can be solved for. After completing these steps the thrust force was found to be:

$$T = \frac{W(\sin\theta - \mu\cos\theta)}{(\sin\alpha + \mu\cos\alpha)} \quad (1)$$

Where W, is the weight of the robot, θ is the degree of the surface angle, α is the thruster angle and μ is the coefficient of static friction.

I B 2) Traversing Irregular or Rough Surfaces

Once adhesion can be obtained successfully robots face another issue, surface roughness or irregular surfaces. While rough surfaces might work to increase friction, which would help adhesion, it also works to lower the normal force that a pneumatic based robot can provide. This is mostly a problem when the climbing surface is not ferro-magnetic, so magnets cannot be used, and the surface has many large cracks, bumps, or geometric patterning. In these cases robots that use suction cups or negative pneumatic adhesion would lose their adhesion due to air entering through the uneven area [16], [9], [17], [18].

Surface roughness mostly affects robots that must make use of careful sealing in order to maintain their adhesion. Depending on the type of robot, brick walls or rock-faces would contain sufficiently rough surface characteristics to cause a catastrophic loss of adhesion. Many pneumatic based robots have overcome the risks of traversing over small surface irregularities by including “skirts” that use bristles or rubber strips [17], [19], [18], [9].

In other cases a robot is required to transition from one surface to another. Examples include floor-to-wall, wall-to-wall, and wall-to-ceiling. During these transitions large air gaps are formed between the robot and the wall that would cause the robot to lose adhesion. In many situations this is mitigated through an active transitioning mode that necessitates the robot to have multiple bodies that can rotate relative to

one another [19], [20], [21]. This type of transitioning can be broken into two categories, interior angle transitioning and exterior angle transitioning. Transitioning can become especially tricky when the new surface doesn't extend very far, like a tall protruding fin. In these cases multi-body robots may be the only solution.

This area is very applicable to the testing standards for Urban Search and Rescue (USAR) robots. USAR mobile robots are regularly tasked with traversing over irregular surfaces to survey areas and reach their desired waypoints. Common applicable goals include climbing up a slope, climb up an obstacle, climb over debris, and passing over a trench [22], [23], [24]. Many of these tasks are meant to simulate conditions where fallen debris has created an obstacle between the robot and the desired position. In the cases where the obstacle cannot be circumnavigated, the robot must pass over it or under it.

I B 3) Robot Climbing Speed

Many times it is not good enough for the robot to simply climb a structure and carry a payload; it must be done in a timely manner. Many climbing robots report their speeds and try to achieve the fastest climbing time. A strong normal force can put excess strain on the motors and can even cause the robot to become stuck [18]. Here, the robots with a naturally high coefficient of friction have the advantage, as well as wheeled based locomotion.

I B 4) Increasing Robot Robustness

Once robots have a climbing ability, they face many other challenges such as safety from falling, control, maneuverability and payload capacity. The need for more robust control and self-sufficiency lets the robot transition from the realm of something that the user must take care of to something that can take care of the user.

I C Problem Definition

To be successful a climbing robot should first be able to climb a wide variety or surfaces. Surfaces can be characterized with a coefficient of friction μ, and a roughness value R_a, and R_z. Coefficients of friction vary from surface to surface and can even vary across the same surface. A good place to start with friction would be concrete. The coefficient of friction between rubber and dry concrete has been reported to be around 1.0 [25], [26]. The coefficient of sliding friction is much more often reported and has been found to be between 0.59 and 0.92 [27], [28].

Outdoor surfaces are regularly exposed to rain and when wet have a lowered coefficient of friction value. Once wet, the coefficient of friction between the two materials drops to a range of 0.45 to 0.75 [26], [28] making it harder to retain adhesion. In one case, a climbing robot was unable to adhere to a surface if there was rain or snow present [29]. Rain water on the surfaces acts as a lubricant which makes sliding much easier which is not desirable when the robot needs to adhere to that

surface. Since wet concrete is harder to climb because of the lowered coefficient of friction value, it is desirable for robots to be able to adhere to surfaces that have the lowest coefficient of friction between it and the robot. To an extent, surfaces with a low μ can be adhered to by using a large normal force. The lowest μ value between the robot and a surface sets the limit as to what the robot can climb. As μ increases for different surfaces the same adhesion force can be attained with a lower normal force which means a smaller effort on the part of the robot.

Rough surface geometry poses a problem for pneumatic based robots. If the robot relies on vacuum or vortex forces, where air has to be moved at a high velocity, a gap between the robot and the surface can change the characteristics of the airflow and therefore reduce the force. Surface roughness is usually measured with a R_a and R_z value where R_a is the arithmetic mean of the surface roughness and R_z is the maximum height of the roughness value [30], [31], [32]. These measurements are normally reported in micro-meters as they are meant to measure very subtle surface features. In this paper they will be used to measure very large and course textures and so the numbers will be quite large. The goal of climbing on rough surface textures is due to the fact that pneumatic based climbing robots can lose their adhesion on these types of surfaces and fall.

A lot of times simply climbing the surface is not enough, the task must be accomplished quickly. Robot speed isn't normally an issue on its own however when

coupled with the task of climbing, it can be very challenging. In the case of legged robots this is particularly difficult as opposed to wheeled or track based robots. Legged robots must quickly place the leg, sometime check to ensure adhesion at that point and then move on to the next leg as part of a walking gait. For wheeled or track based robots, the adhesion mechanism is working all the time and the robot simply drives the way another robot might drive on the floor. The measurement of speeds can vary but it is usually measured in cm/s.

In Chapter II the different abilities of existing robots will be discussed. What is apparent is that lots of robots are designed for specific tasks or climbing surfaces. In many cases the entire focus of the research has solely been the climbing ability, worked on by multiple researchers. The aim of this project will be to increase the ability of a climbing robot.

There are two USAR testing conditions that can be applied to the climbing robot performance experiments. This first is traversing over a trench of a given width and depth [22], [23]. Normally the depth of the trench would not matter however in the case of pneumatic adhesion it can make all the difference. For many robots that use negative pneumatic pressure a narrow, shallow trench does not let enough air through to cause any losses of adhesion. However a large gap could result in a catastrophic loss of adhesion and cause the robot to fall. Even a very narrow gap what was very deep would cause great losses.

The issue of surface gaps arises in the task of climbing on extremely rough surfaces where there may be lots of places for air to rush into the low pressure zones inside the robot. A direct trench test would also be beneficial where gap widths and depths can be easily measured in units of millimeters.

The second testing condition for USAR robots is the ability to overcome obstacles. Sometimes this is as simple as climbing up a ramp [24] or climbing over an obstacle that might necessitate the robot to transition through a given angle [23]. An experiment to test this condition would involve two planes that could be rotated relative to one another for a measured angle. The robot would attempt to transition between them until it could no longer do so. Paremeters would be measured in degrees.

I D Assumptions

Since this research is being conducted with limited time and funding, certain simplifying assumptions will be made.

- Only the characteristics of pneumatically based robots will be considered.
- All types of locomotion will examined however wheeled will be chosen.
- Any outdoor climbing will occur in good weather (not raining).
- Ability to carry large payloads will not be considered in this study.
- Tethered operation of the robot is an acceptable option.
- Only concave surfaces will be experimented on.

- Experiments with unique surface qualities such as specified gaps will use MDF board as the surface for its low cost and ease to work with.

I E Constraints

Component wise the greatest constraint is on the adhesion method. If it is desired for the robot to be in position for a great length of time, then it is necessary for the adhesion method to not consume any power. With this in mind the best techniques are either a lighter-than-air robot that could float to the desired location, or a climbing robot that uses a dry fibular adhesive.

The former method isn't exactly a climbing robot but is certainly a service robot. A previous study conducted revealed that the required volume would be too large to be practical. Dry fibular adhesive would be the ideal choice for extended runtime however the material is very expensive, hard to find, and harder to manufacture.

Some experiments will only be done with a certain material. This will constrain the range of coefficients of friction however it can be assumed that specifications obtained at a given μ will also be present at higher values of μ.

I F Objectives

The objectives for this research are:

- Design a pneumatic based adhesion method that will allow a robot to stick to a concrete, brick, glass and other such surfaces.

- Climb on a surface with the lowest possible coefficient of friction between it and the robot. Primarily, it is desired to climb on a surface with a friction coefficient of less than 0.74.
- Be able to overcome a step-like obstacle with a height of greater than 10mm while climbing.
- Use a single body robot to passively transition through a sharp surface changes both from the ground and while climbing.
- Have the ability to traverse over a gap-type obstacle while climbing without loss of adhesion or mobility.

II LITERATURE REVIEW

II A Adhesion Mechanisms

Many different adhesion mechanisms exist for climbing robots. These include suction force, magnetic force, gripping/penetrating force, compressive friction, trust force, and the most modern popular choice, dry fibular adhesive, [1], [2], [3], [4], [9], [33]. Gripping or penetrating force works well when the climbing surface is a cylindrical pole as is the case for the wind turbine inspection robot by Sattar and Rodriguez, [2]. Another example is in the case of climbing telephone poles, were the surface is relatively soft and there is not much concern for light damage, this is the case for the RiSE V3 Robot by Haynes *et al*. [3].

In other cases the surface is ferro-magnetic and therefore the robot can employ permanent magnets to adhere. This is usually accomplished through non-contact as there would be too much friction induced and the robot would not be able to move. The Company Helical Robotics employs such a mechanism [5], as well as the RVC robot that uses four legs with permanent magnets on a peeling pad, [9] [34]. Often, robots that employ magnetic or suction adhesion have the greatest payload carrying capacity [9].

By far the most popular modern adhesion mechanism is dry fibular adhesive, also known as gecko feet. This method is very complex and involves manufacturing special

pads with micro-level features [12]. Methods that can accomplish this include micro-molding, nano-embossing, carbon nanotube growth, and lithography [35], [14]. These pads can have the unique ability of adhering well when forced in one direction and then peeling off easily if forced in another [33], [36]. However as stated before, these pads are extremely difficult to manufacture and their creation alone is subject of many papers.

II B Robots Using Negative Pneumatic Pressure for Adhesion

Lots of existing climbing robots make use of negative pneumatic pressure as their method of adhesion including robots by Sekhar *et. al.* and Yoshida *et. al.* [37], [38]. There are many ways to gain and maintain suction force, each with their benefits and drawbacks. The first is to carry a compressor or vacuum pump on the robot to provide adhesion. While this is capable of producing large adhesion forces it adds a lot of bulk and weight to the robot itself. Additionally it can take time to produce the suction force which limits the speed of the robot [1]. It is also possible for suction to be lost while traveling over uneven or cracked surfaces. In some cases it has been reported that the robot can shift and loose adhesion due to suction cup deformation [10].

A slightly different method is to use an impeller to create a low pressure region underneath the robot that results in adhesion [1], [4]. An example of this is the robot LARVA II by Koo *et al.* [16]. These types of robots have the benefit of using wheeled motion resulting in quick maneuverability. Additionally these robots do not exactly

need a perfectly smooth surface to adhere to. Draw backs include constant power consumption, inability to cope with obstacles, and excess noise generation. Another robot named CROMSCI by Schmidt makes great use of pneumatic force for adhesion however used a tethered power system [18]. The Alicia II robot by Francisci *et. al.* also makes use of low pressure regions generated by the robot to obtain surface adhesion [17]. It was mentioned that small irregularities or obstacles could cause the internal pressure to rise thereby resulting in an overall loss of adhesion. In addition, if the system were to drop the pressure too low the adhesion forces would be so strong that the robot would not be able to move due to high friction forces [17].

Wall climbing robots such as CROMSCI and City Climber use closed loop control systems to monitor the adhesion force of their robots [18] [19]. In the case of CROMSCI, control is achieved by actuating valves that control the amount of air moving through the robot [18]. By closing valves, the suction force is limited and therefore adhesion is either strengthened or reduced. In addition City Climber utilizes in-body pressure sensors to monitor low pressure zones [19].

To prevent catastrophic rises in internal pressure, most pneumatically based robots make use of “skirts” which are flexible barriers around the robot body that flex over surface irregularities and allow the robot to keep a low internal pressure [16], [17], [18], [19]. These skirts are very effective when faced with small protruding obstacles. However the skirt cannot do anything when the robot traverses over a large, deep

crack. In these cases the robots become vulnerable. Large recessed features that are very deep, but much smaller in width than the size of the robot, can let large amounts of air in and disrupt the low pressures adhering the robot to a surface [17], [39].

II C Mobility Over Irregular Surfaces

Rough surfaces are difficult in general for mobile robots but are especially crippling for climbing robots. As stated before the surface roughness is measured with a R_a and R_z value where R_a is the arithmetic mean of the surface roughness and R_z is the maximum height of the roughness value [30], [31], [32]. These numbers have the units of micrometers and are usually measured with special equipment. In this study only very rough surfaces will be examined which are surfaces that have R_a values of over 50 or 0.05 mm. In this range the measurement can be gathered with calipers. The ability to travel over extremely rough surfaces is important because this is a major obstacle for pneumatically based robots that can possibly lose adhesion on these surfaces.

The robot city-climber by Xiao *et.al.* has reported that its robot can climb surfaces with a maximum step clearance of 1 cm [39]. They go on to report that their robot is capable of climbing brick, wood, glass, stucco, plaster, gypsum board, and metal [39]. This variety of surfaces poses two challenges, the first being the ability to climb a smooth surface such as glass and the second being able to climb the rough surfaces. As stated in previous sections the coefficient of friction μ is the major determining

factor on whether a robot can or cannot adhere to a particular surface with a given normal force. This particular robot uses negative pressure to generate its normal force and has a skirt of flexible bristles to help cope with irregular surface geometry and maintain low internal pressures [39]. The maximum step size clearance that they report is the equivalent of a R_z value of 10,000. While they also claim that the robot can cross over surface gaps while climbing they do not specify how wide or how deep.

In addition to a skirt the robot, LARVA-II by Koo *et.al.,* uses a suspension system on its wheels to help overcome surface irregularities [16]. This is a clever idea that has its own drawback. While being an improvement in that a peg or bolt head would not tilt the chassis so much that the robot would lose adhesion, this will only be of benefit when the obstacle sticks out of the surface rather than indented. With the suspension system aiding in mitigating small infrequent obstacles, the sealing pad still needs a relatively smooth contact surface. It was, however, able to climb a concrete surface with its own surface cracks, chips, and holes [16]. During one test the robot traversed a surface with a peg protruding 8mm out of the surface. In this test the robot's wheel was successfully able to roll over the peg while the robot itself maintained adhesion. This would correspond to a R_z value of 8,000.

Like the robot city-climber, the robot Alicia 3 was designed to overcome obstacles in the range of 1 cm to 10 cm [17]. However this is only accomplished with a multi-body system, specifically three bodies. The robot uses pneumatic pistons to lift each

individual body up and over the obstacle in question [17]. Along the sealing pad, the robot can traverse over surfaces that have irregular features less than 1 cm such as screws or surfaces with a R_z value less than 10,000.

Robots such as the quadruped MRWALLSPECT III use suction pads on the ends of four mechanical legs. While the robot is able to climb over obstacles since it uses a sealing pad, it can be assumed that each leg must contact a surface that is relatively smooth. Another example by Sekhar *et.al.* can climb glass, metallic surfaces, wood and concrete [37]. While it was stated that the robot could climb rough surfaces, there was no stated measurement for how rough the surface is.

Gaps and trenches pose another potential fatal obstacle for climbing robots. Wheel based robots using pneumatic adhesions can experience a loss of pressure differential once the robot has moved over a gap or crack large enough to allow a significant amount of air through. In a report by Leibbrandt et. al. it was stated that while their robot was able to move on concrete surfaces, it was desirable for the robot to pass over a gap of greater than 2cm [40]. Thus it has been recognized that these types of obstacles can possibly pose great problems for climbing robots and that it is a desirable problem to solve.

II D Robots Using Thrust for Adhesion

There are a few existing examples of thrust based adhesion. One example is the Holonomic Motion Vehicle for Travel on Non-Level Surfaces by Troy *et al.* [41]. Another robot that uses thrust force was referenced in a Robotics and Automation Journal, [9] where the robot made use of two propellers to generate thrust force and then used wheel for locomotion. According to the article the robot was very unstable which hindered further research [9].

An interesting thrust based robot developed by Shin et al. is part UAV, part climbing robot. The robot is setup like a quadcopter but with wheels in addition to propellers. It can convert from flying mode to climbing mode by bumping into a wall and then flipping itself up by accelerating rear thrusters [42].

II E Climbing Speed for Pneumatically Based Robots

Climbing speed is another important factor for climbing robots as it is desirable for the robot to get to the target location quickly. In this area wheeled or track based robots have a major advantage to legged based robots. The fast mobility of a wheeled robot makes up for the fact that it will have a harder time overcoming obstacles. Another advantage is that wheeled systems can easily be converted into track systems and are simply driven by DC motors while legged systems have many motors and use complex walking algorithms.

The robot NINJA 1 by Hirose *et.al.* is a leg based climbing robot that uses negative pneumatic pressure at the ends of each leg to attain adhesion [43]. It was reported that this robot has a maximum climbing speed of 20 mm/s in the vertical direction and 50 mm/s in the horizontal direction. While this robot does have a large natural reach, it is still limited by the mass of its legs. Another robot with walking motion is the robot MRWALLSPECT III by Kang *et.al.* that uses a set of four legs tipped with multiple active suction cups [8]. The robot has relatively high mobility in being able to overcome obstacles and it was reported that it has a maximum walking velocity of about 50 cm/min.

A wheeled example of a climbing robot is City-Climber, which uses an active impeller system to generate negative pressure inside a chamber of the robot. This robot uses a bristled skirt around the perimeter of the robot to act as a deformable barrier to help hold in air. The wheels that drive this robot are underneath this skirt inside the vacuum chamber. An impressively robust robot, City-Climber is able to climb on rough surfaces and even transition between surfaces if it has at least two bodies connected through and actuated arm. The maximum climbing speed of this robot is 10 m/min [39].

A similar robot is the robot LARVA which uses a similar active impeller system to generate low internal pressures and there-by attaining surface adhesion. Also similar to many other negative pressure chamber robots, it uses a flexible skirt to help cope

with uneven surface geometries. The drive system of this robot consists of two DC motor driven wheels and a passive ball castor all outside of the suction zone. This robot is able to travel up a wall at a maximum speed of 12 cm/s with this configuration [16].

Finally a robot by Daniel Schmidt called CROMSCI also used DC motor driven wheels while along with impeller driven suction. This robot in particular uses a sophisticated system of load cells, gearboxes, encoders and motors, all in a compact configuration inside the vacuum chambers of the robot. The driving motor in this system is actually a torque motor, which makes it easier to mount inside the wheel assembly. CROMSCI, with the configuration stated, has a maximum climbing velocity of 9.63 m/min [18]. A survey of climbing robots by Schmidt and Berns suggests that climbing robots should be able to achieve a velocity of at least 10 m/min to be useful [9].

II F Summary

The existing abilities of climbing robots are summarized in Table 1, Table 2, and Table 3 below. These are based on a literature review into climbing robot abilities.

Climbing Robot	Adhesion Method	Very Smooth Surfaces (R<0.2)	Semi Smooth Surfaces (0.2<R<20)	Rough Surfaces (20<R <2000)	Very Rough Surfaces (R>2000)	Magnetic Surfaces	Meshed and Porous Surfaces
RAMR2 [44]	Suction Cup – Active	X	?	?		X	
MRWALLSPECT III [8]	Suction Cup – Active	X	?	?		X	
City-Climber [19], [39]	Vacuum Impeller	X	X	X		X	
NINJA-1 [5]	Suction Cup – Active	X	X	X		X	
CROMSCI [18]	Vacuum Impeller	X	X	X		X	
Raccoon [9]	Suction Cup – Passive	X				X	
Alicia II [17]	Vacuum Impeller	X	X			X	
LARVA [16]	Vacuum Impeller	X	X	X		X	
Nishi Robot [9]	Thrust Force	-	-	-	-	-	-
CR4	Thrust Force	X	X	X	X	X	X

Table 1: Surface Climbing Ability of Different Robots

Climbing Robot	Adhesion Method	Locomotion Method	Ability to Transition Between Surfaces (Single Body)
RAMR2 [44]	Suction Cup – Active	Legged-Biped	X
MRWALLSPECT III [8]	Suction Cup – Active	Legged-Quadruped	X
City-Climber [19], [39]	Vacuum Impeller	Wheeled	-
NINJA-1 [5]	Suction Cup – Active	Legged-Quadruped	X
CROMSCI [18]	Vacuum Impeller	Wheeled	-
Raccoon [9]	Suction Cup – Passive	Wheeled	-
Alicia II [17]	Vacuum Impeller	Wheeled	-
LARVA [16]	Vacuum Impeller	Wheeled	-
Nishi Robot [9]	Thrust Force	Wheeled	-
Alicia III [17]	Vacuum Impeller	Legged/ Wheeled	-
CR4	Thrust Force	Wheeled	X

Table 2: Robot Surface Transition Abilities (Angle Ranges Not Specified)

Climbing Robot	Adhesion Method	Locomotion Method	Step Height Clearance
City-Climber [19], [37]	Vacuum Impeller	Wheeled	10mm
LARVA [16]	Vacuum Impeller	Wheeled	8mm
CROMSCI [18]	Vacuum Impeller	Wheeled	6mm
Alicia II [17]	Vacuum Impeller	Wheeled	10mm

Table 3: Climbing Robot Step Clearance Survey for Wheeled Robots

II G Potential Contributions

Completion of this research will potentially generate new knowledge and innovation into the area of climbing robots. A summary of objectives and their respective contributions are shown below in Table 4.

Objective	Contributions
Design a pneumatic based adhesion method that will allow a robot to stick to a concrete, brick, glass and other such surfaces.	Use of new air ducts, impellers, propellers, or motors could increase maximum potential surface adhesion.
Climb on a surface with the lowest possible coefficient of friction between it and the robot. Primarily, it is desired to climb on a surface with a friction coefficient of less than 0.74.	It is very difficult for a robot to climb a surface where the value of μ between the robot and the surface is low. A versatile robot, therefore, should be able climb surfaces with low values of μ.
Be able to overcome a step-like obstacle with a height of greater than 10mm while climbing.	This would show robustness and the ability to maintain adhesion in the case of encountering obstacles while in climb. Other protrusions and obstacles may also inhibit the robot's ability to climb, especially if they cause a significant air gap. The robot City Climber can climb over surfaces with a step clearance of 10mm [39].
Use a single body robot to passively transition through a sharp surface changes both from the ground and while climbing.	Passing between surfaces with sharp angles can cause an increased air gap beneath the robot and cause robots that use negative pneumatic adhesion to lose adhesion at the transition, potentially causing the robot to fall. Single body robots will reduce cost and complexity. This type of test is typical for USAR robots.
Have the ability to traverse over a gap-type obstacle while climbing without loss of adhesion or mobility.	Using a different configuration it is desired to show that not only will the robot be able to maintain adhesion over gaps or trenches, it will be able to pass over them and continue climbing. The greatest weakness of pneumatic based robots that use negative pressure for adhesion is climbing over gaps in the surface where air might enter and cause the robot to loose adhesion. The ability for the robot to passively travers over a trench while climbing and doing so without the use of multiple platforms allows for simpler algorithms and easier user control as well as faster climbing. This type of test (ground based) is typical for USAR robots.

Table 4: Potential Research Contributions

III EXPERIMENTAL DESIGN

To accomplish the objectives set forth in section I F, multiple of experiments will be created to test and evaluate individual abilities. These tests will be used to configure and calibrate sensors and motors, as well as determine the specifications for the final robot. As for location, many tests will be performed in a small lab but other tests will require other locations to test certain environmental conditions such as different climbing surfaces.

III A Preliminary Experiments: Verification of Theory

III A 1) Objective

This is the first of a set of experiments that will be used to determine the performance specifications of the climbing robot CR4. The purpose of the preliminary tests will be to measure certain parameters on both the robot and the test rig that will be used in later experiments.

The first experiment determined the coefficient of friction between the robot and each of the climbing surfaces that were tested. Not only was this used in verifying the theory but provided a baseline for real world applications for this robot configuration.

The second experiment was concerned with measuring the actual thrust output of the fan. As is, the user adjusts a slider in the smart phone application that sets a PWM

duty cycle. The duty cycle set controls the fan speed and so a mapping of slider percentages to actual forces is needed.

Finally, theoretical thrust values were calculated and then compared to measured values of a given surface type, surface angle, and thrust angle.

III A 2) Procedure and Setup

This first test measured the coefficient of friction μ between the robot and a given surface in a very standard way. This standard method involved placing the robot on a given surface and then slowly tilting the surface at an angle. The surface continued to be tilted until the robot slipped and the slip angle recorded. The tangent of the angle before the slip occurred is the measured coefficient of static friction [45] [46] [47]. A smart-phone running a protractor app was used to display the current angle of the surface as it was tilted. To hold the phone, a stand was 3D printed so that it could remain stationary relative to the surface. This setup can be seen in Figure 2.

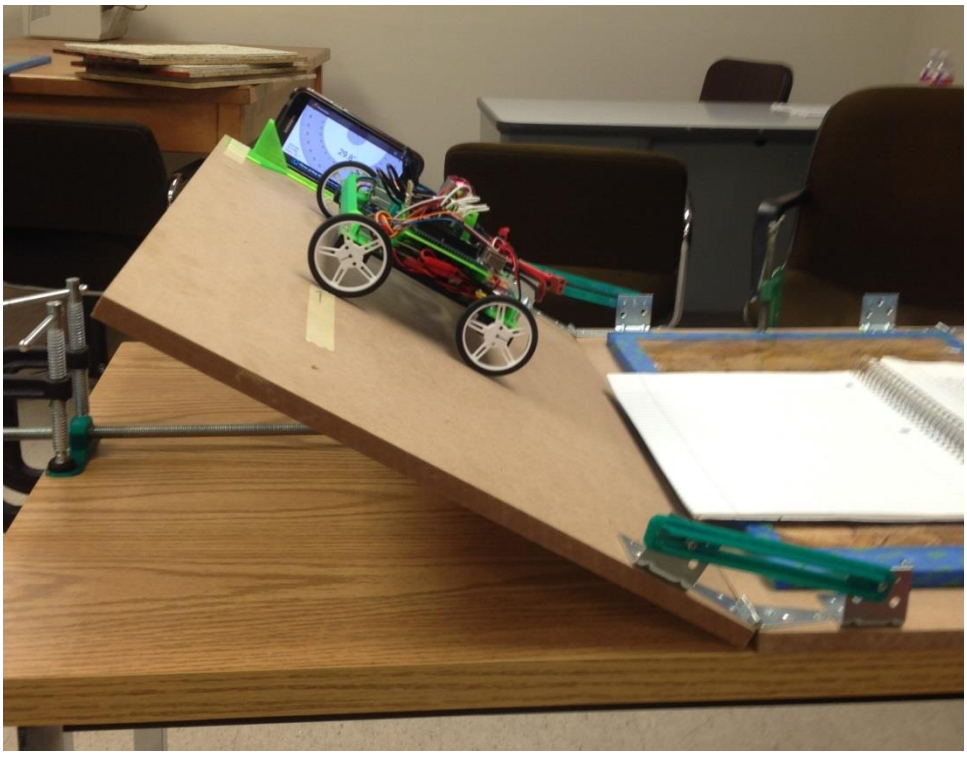

Figure 2: Experimental Setup - Measuring Friction

Measuring the thrust force involved creating a test rig in CAD and then manufacturing and assembling the components. The experiment used the ducted fan to deflect a cantilever and a strain gauge. This is a common setup used in small digital scales to measure light-weight items and so it will be replicated. A picture of the set-up is shown below in Figure 3 and Figure 4.

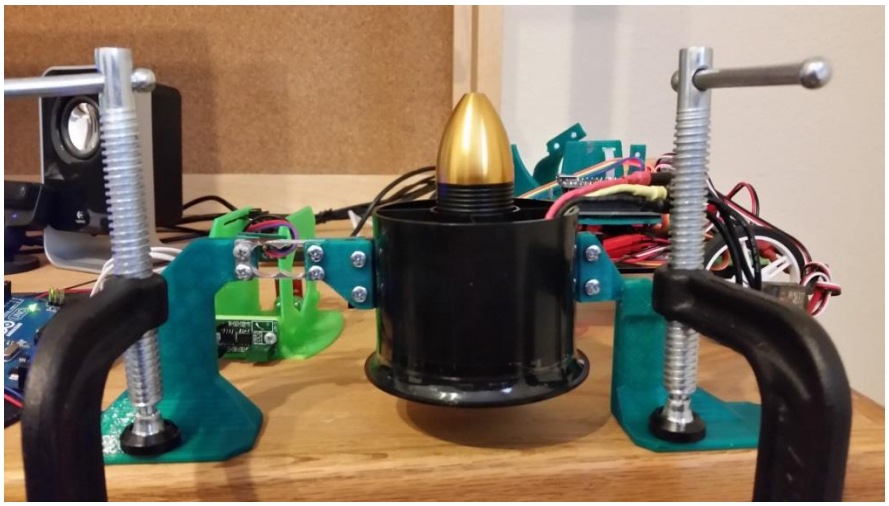

Figure 3: Full Thrust Stand Setup

Figure 4: Aluminum Cantilever Beam with Strain Gauge

The thrust stand and strain gauge were first be calibrated by placing fishing weights of known mass on a 3D printed cup that was placed over the center of the fan motor. As weights were added, amplified signals from the strain gauge were read and displayed using an Arduino Uno. Once calibrated the fan was then connected to the electronic

speed controller of the climbing robot. In this way one microcontroller could be used to collect data from the strain gauge and the other could be used to set the fan speeds through the controller app. Values were obtained for two batteries, an 11.1V battery and a 14.8V battery.

11.1V Battery	20%	30%	40%	50%	60%	70%
Average Thrust	-	-	-	-	-	-

Table 5 and Table 6 show the desired value ranges.

11.1V Battery	20%	30%	40%	50%	60%	70%
Average Thrust	-	-	-	-	-	-

Table 5: Digital Scale Measurements for Thrust (11.1V)

14.8V Battery	20%	30%	40%
Average Thrust	-	-	-

Table 6: Digital Scale Measurements for Thrust (14.8V)

III A 3) Materials Needed

- Glass Test Surface
- MDF Test Surface
- Brick Test Surface

- Concrete Test Surface
- Test Platform with Adjustable Angles
- Smart-phone with Protractor App
- Test Stand for Smart-phone
- Stain Gauge and Amplifying Circuit
- Arduino Uno (For Receiving Data)
- Thrust Stand
- Climbing Robot

III B Experiment 1: Adhering to Surfaces with Various Coefficients of Friction

III B 1) Objective

The objective of the first experiment was to be able to climb on a surface with the lowest possible coefficient of friction between it and the robot. Primarily, it was desired to climb on a surface with a friction coefficient of less than 0.74.

III B 2) Hypothesis

Ho: The robot will adhere to surfaces with coefficients of friction greater than or equal to 0.74 between the robot and the surface.

Ha: The robot will adhere to surfaces with coefficients of friction less than 0.74 between the robot and the surface.

III B 3) Problem Area: Adhering to a Vertical Surface

The first problem area for climbing robots is simply adhering to the desired surface. From Figure 1 it can be seen that friction and adhesion forces are what hold the robot onto a surface. As angles get larger with respect to the vertical adhesion forces play a larger role but for relatively vertical surfaces, adhesion is driven by the coefficient of friction μ. Thus it is very difficult for a robot to climb a surface where the value of μ between the robot and the surface is low. Certain qualities such as the roughness of the surface or whether the surface is wet or dry will influence how well the robot will perform. A versatile robot, therefore, should be able climb surfaces with low values of μ. In a test of measuring the value of μ between a rubberized pad and wet vs dry concrete by the Russ Engineering Group, it was found that the average μ between the pad and dry concrete was 1.02 while the average value of μ for wet concrete had dropped to 0.74 [26]. In all tests, the value of μ did not drop below 0.53.

III B 4) Procedure and Setup

To show basic climbing ability, the robot performed twenty-five timed climbing trials on each surface of interest. Each climb was 500mm in length to ensure that there was enough distance to demonstrate positive climb without any doubts while not draining the battery excessively. This allowed for more trials before the robot must be recharged. At the start of each trial, the robot started from rest at the ground level and transitioned into a climb up to the 500mm height. The duration of the climb was

timed using a stop-watch app installed on a tablet. This setup is shown below in Figure 5.

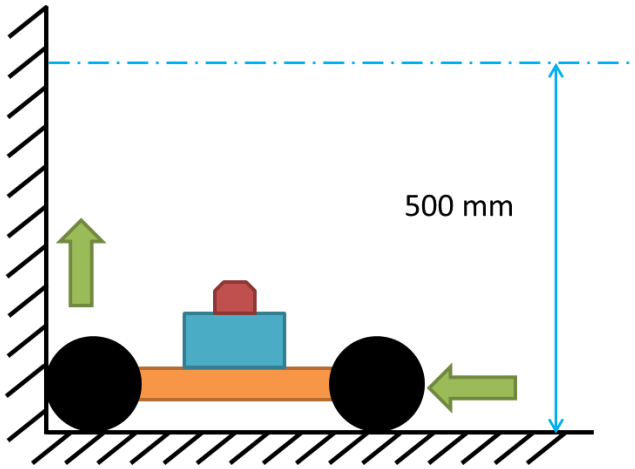

Figure 5: Experimental Setup - 500mm Climb

The actual experimental setup can be seen in Figure 6.

Figure 6: Experimental Setup – Glass, MDF, Brick, and Concrete Climbing Surfaces

Data was collected to be displayed in section 0 in the format seen in Table 7 and Table 8.

Material	Average Thrust Force Required
Glass	-
MDF	-
Brick	-
Concrete	-

Table 7: Experiment 1 - Thrust Force Data to Be Collected

Material	Average Thrust Angle Required
Glass	-
MDF	-
Brick	-
Concrete	-

Table 8: Experiment 1 - Thrust Angle Data to Be Collected

III B 5) Materials Needed

- Glass Test Surface
- MDF Test Surface
- Brick Test Surface
- Concrete Test Surface
- Test Platform with Adjustable Angles
- Stopwatch or Stopwatch App.

III C Experiment 2: Climbing Over Obstacles (Step clearance > 10mm)

III C 1) Objective

It was desired for the robot to be able to climb over a step-like obstacle with a height of greater than 10mm while climbing. This would show robustness and the ability to maintain adhesion in the case of encountering obstacles while in climb.

III C 2) Hypothesis

Ho: The robot will be unable to climb on surfaces with a protrusion of greater than or equal to 10mm.

Ha: The robot will be able to climb on surfaces with a protrusion of greater than 10mm.

III C 3) Problem Area: Irregular Surface Geometry.

In continuing on the problem area of adhering to surfaces, one persistent challenge of pneumatically based climbing robots is their ability to climb on very rough surfaces. Any gaps that lead to air leaks will cause the robot to loose adhesion if the adhesion system relies on suction. An R value of greater than 50 refers to a greater roughness than is on most typical surface finishing charts. Since this value is measured in micrometers a maximum surface height change of 1mm would yield an Rmax value of

1000. As surfaces become very rough, it becomes increasingly difficult for suction based robots to maintain adhesion.

Other protrusions and obstacles may also inhibit the robot's ability to climb, especially if they cause a significant air gap. While legged robots can step over these obstacles a wheeled robot may be forced to drive over them. In the case of the walking robot or the wheeled robot that uses multiple carts that are connected through an actuating arm, the height of the obstacle that must be traversed is dependent on the length of the arm or leg. In this case the focus will be on the abilities of a single, wheeled cart.

The robot City Climber can climb over surfaces with a step clearance of 10mm [39] while the robot LARVA II can climb over surfaces with a step clearance of 8mm [16]. The robot CROMSCI can climb over surfaces with a step clearance of 6mm [18]. ALICIA II can climb over surfaces with a step clearance of less than 10mm [17].

III C 4) Procedure and Setup

Obstacles of a set height were fixed in the climbing path of the robot. Once again the robot needed to make a 500mm climb while traversing over the obstacle. Twenty-five timed trials took place and the times were averaged together. Once twenty-five trials were completed, the obstacle height was increased by 5mm and the experiment repeated.

A “speed bump” like obstacle was created using a 3D printer and then fixed to a piece of MDF with screws. To increase the height of the obstacle 5mm booster pieces were added. The duration of the climb was timed using a stop-watch app installed on a tablet. The general setup for the experiment is shown in Figure 7 with the actual setup shown in Figure 8.

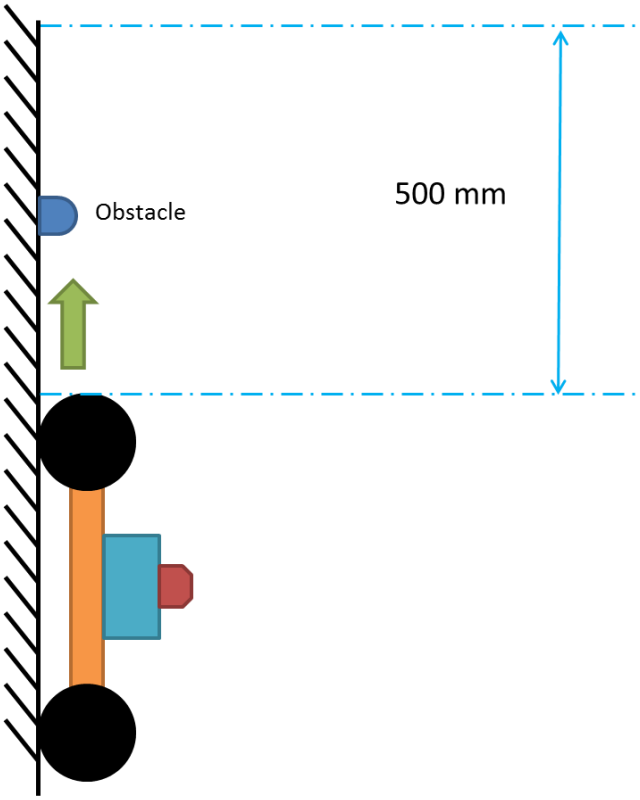

Figure 7: Experimental Setup - 500mm Climb over an Obstacle

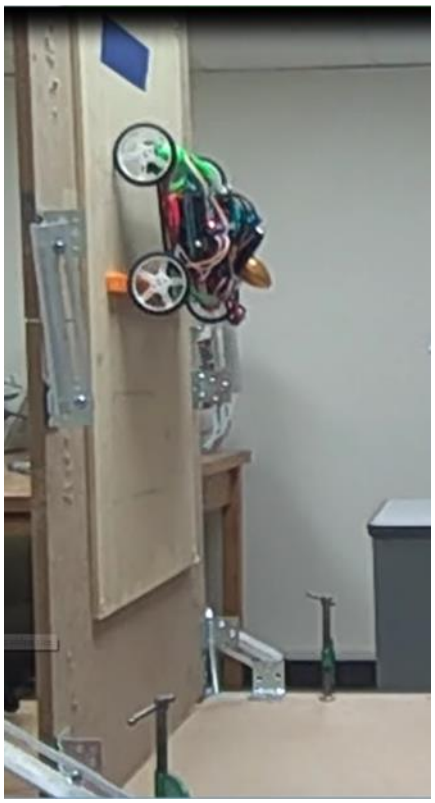

Figure 8: Experiment 2 Actual Setup with 15mm Obstacle

Data for the experiment was collected in the following format shown in Table 9.

h	Time (Avg.)	Thrust % (Avg.)	Thrust Angle α (Avg.)
5mm	-	-	-
10mm	-	-	-
15mm	-	-	-

Table 9: Experiment 2 - Thrust Data to Be Collected for Various Protrusion Heights

III C 5) Materials Needed

- MDF Test Surface
- Test Platform with Adjustable Angles

- Stopwatch or Stopwatch App.
- (15mm x 180mm x 5mm) step pieces (x6)

III D Experiment 3: Passive, Single Body Surface Transitioning

III D 1) Objective

In this experiment it was desirable for the single body robot to passively transition through a sharp surface change. Passing between surfaces with sharp angles can cause an increased air gap beneath the robot and cause robots that use negative pneumatic adhesion to lose adhesion at the transition, potentially causing the robot to fall. This is normally overcome by using two bodies that are actuated so that one body always can maintain adhesion on a surface. The design goal of CR4 was to be able to accomplish this with a single body.

III D 2) Hypothesis

Ho: The robot will be able to passively transition through a surface angle of greater than or equal to 90° with the horizontal.

Ha: The robot will be able to passively transition through a surface angle of less than 90° or there will be a lower limit, beyond horizontal that the robot could pass through.

III D 3) Problem Area: Inverted Angles and Irregular Geometry

A common test in USAR robotics is the ability to traverse on irregular surfaces. Many times this includes random debris but also includes things like ramps and uniform obstacles [24]. For most land robots without climbing ability there is a maximum inclination were it would be too steep for the robot to traverse successfully.

III D 4) Procedure and Setup

For this scenario angles were measured from the horizontal where 180° was perfectly flat, 160° was a shallow ramp, and 90° was a vertical wall. Testing this involved a setup of hinged surfaces with different surface finishes. Concrete was created from a mix and applied over a wire mesh onto a plywood surface. Glass panels were also used to simulate very smooth surfaces at various angles. Glass panels can be bought at a local hardware store and they can be attached to plywood with adhesive and then screwed to the test rig. These materials will help represent the range of industrial surface finishes likely to be encountered.

The surfaces were locked at specified angles while the robot attempted to transition through them. This was accomplished by pivoting bracing arms on mounting brackets between two surfaces. If the robot is able to pass from a horizontal surface to an inclined surface while maintaining adhesion then the test will be successful. A smart phone with a protractor application will be used to measure the inclined angle. Also

the coefficient of friction between the robot and the surface will be measured beforehand as was done in previous experiments.

Angles were adjusted in 20° increments until the surface is at 90° and then was adjusted in 10° increments. If one angle proves to be harder than the other, the problem angle will be held at its limiting value while the remaining angle is adjusted. Twenty-five timed trials were run for each configuration and the trial was considered a success if the robot is successfully able to pass through both angles. Thrust output percentage and thruster angle were also recorded as they will be set values that favor a successful outcome. Figure 9, Figure 10, and Figure 11 show the designed and actual setup for the experiment. Data will be collected in the format shown in Table 10 and Table 11.

Concrete										
Surface Angle	**150-150**		**130-130**		**110-110**		**90-90**		**80**	
	First Trans.	Second Trans.	First Trans.	Second Trans.	First Trans.	Second Trans.	First Trans.	Second Trans.	First Trans.	Second Trans.
Thrust Force	-	-	-	-	-	-	-	-	-	-
Thrust Angle	-	-	-	-	-	-	-	-	-	-

Table 10: Concrete Surface Transition Result Table

Glass										
Surface Angle	**150-150**		**130-130**		**110-110**		**90-90**		**80**	
	First Trans.	Second Trans.	First Trans.	Second Trans.	First Trans.	Second Trans.	First Trans.	Second Trans.	First Trans.	Second Trans.
Thrust Force	-	-	-	-	-	-	-	-	-	-
Thrust Angle	-	-	-	-	-	-	-	-	-	-

Table 11: Glass Surface Transition Result Table

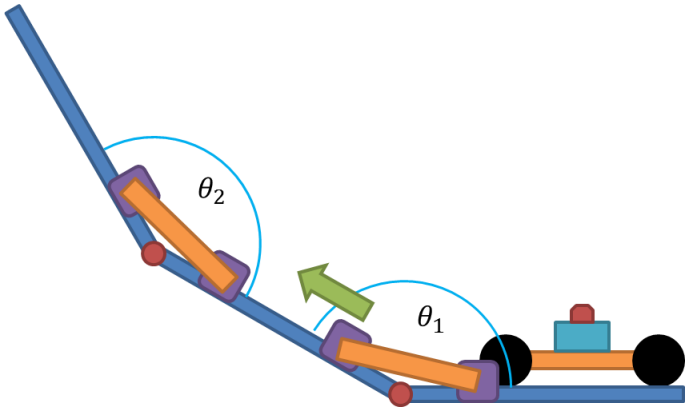

Figure 9: Experimental Setup – Transition through Two Angles

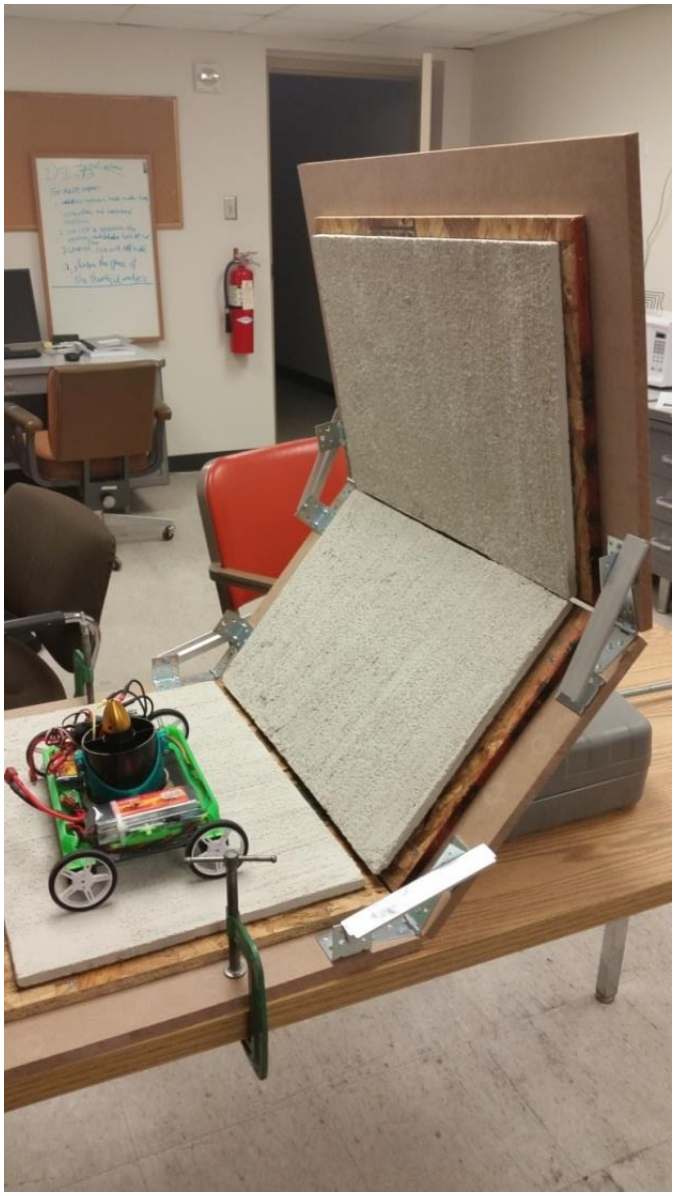

Figure 10: Experiment 3 Actual Setup 130-130 Degree Concrete

Figure 11: Experiment 3 Actual Setup 90-90 Degree Glass

III D 5) Materials Needed

- Glass Test Surface
- Concrete Test Surface
- Test Platform with Adjustable Angles
- Smart-phone with Protractor App
- Test Stand for Smart-phone

III E Experiment 4: Climbing Across a Gap of Known Width and Depth

III E 1) Objective

The objective of this experiment was to have the ability to traverse over a gap-type obstacle while climbing. Large cracks and gaps on the climbing surface can result in loss of adhesion and catastrophic failure of the robot. Using a different configuration, it was desired to show that not only will the robot be able to maintain adhesion over gaps or trenches; it would be able to pass over them and continue climbing.

III E 2) Hypothesis

Ho: The robot will be able to passively climb over a trench that is 55mm wide or less.

Ha: There will be a limit that is less than 55mm which the robot can successfully climb over.

III E 3) Problem Area: Overcoming Obstacles

Another common test in USAR Robotics is the ability to move over a trench [22], [24]. For a ground based robot the trench may be caused by debris or structural damage and vehicles may be required to climb over gaps as wide as 0.01.-0.1m. This is accomplished in a variety of ways from extendable arms to multiple actuated bodies.

The problem becomes a bit more complicated for climbing robots. For instance if the robot uses pneumatic methods for adhesion, whether passive or active, the presence of a small trench such as a crack could cause a catastrophic loss of adhesion if passed over. In some cases where the adhesion method is active, the robot will make use of a flexible skirt in order to minimize the effective gap between the robot and the surface. Using this, robots have been shown to be able to climb brick surfaces where the mortar between bricks might otherwise cause a problem for other pneumatically based robots. However, if this trench were to become sufficiently deep, the loss of the internal pressure differential could cause the robot to lose adhesion on the wall.

The trench could be overcome by either stepping over the problem area in the case of multiple bodies with actuation or passing over the trench simply by utilizing the large geometry of the robot itself. By using thrust based adhesion, the depth of a trench should no longer be an issue and the only remaining concern should be the width of the trench. The desired data to be collected is shown below in Table 12.

Gap in Concrete (23mm Depth)				
Gap Length	**55mm**	**45mm**	**35mm**	**25mm**
Thrust Force	-	-	-	-
Thrust Angle	-	-	-	-

Table 12: Experiment 3 - Thrust Data to Be Collected for Various Gap Sizes

III E 4) Procedure and Setup

This experiment used the simulated concrete surface from the third experiment as its characteristics are known. Two of those panels were clamped vertically to a surface with a gap of known width and depth between them. The robot then attempted to climb through the trench without getting stuck. The experiment was considered successful if the back wheels of the robot are able to make it to the second surface and clear the trench. To verify testing, 25 trials took place for each set-up. After 25 trials were completed for the initial set-up, the trench width will be increased by 10mm and the test will be repeated. This will continue until the robot is no longer able to succeed or it is suspected that the test is likely to cause severe damage to the robot. The set-up for this can be seen in Figure 12 and Figure 13 below.

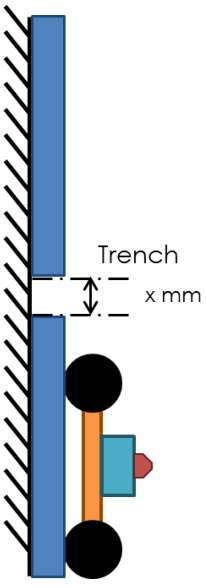

Figure 12: Experimental Setup – Traversing Over a Gap

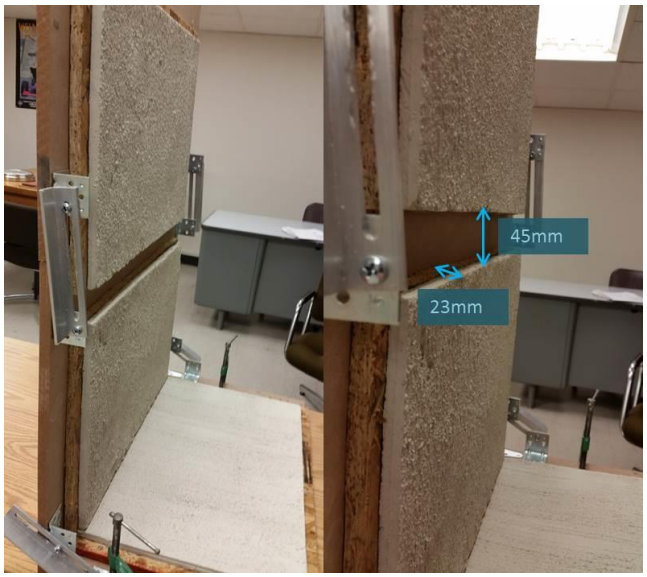

Figure 13: Experiment 4 Actual Setup

III E 5) Materials Needed

- Concrete Test Surface
- Test Platform with Adjustable Angles
- Ruler or Calipers

IV EXPERIMENTAL RESULTS

IV A Preliminary Experiments

Connecting the robot's performance abilities with theoretical calculations adds validity to the experiment and demonstrates mastery over the subject under study. Simple statics based equations were used to help predict the robots behavior on surfaces with a given angle and coefficient of friction and were discussed in section I B. In this section a mathematical model of a climbing robot was constructed for an arbitrary position on a given surfaces with known specifications. This model was then analyzed to show the theoretical thrust required to maintain its static position on a wall. The first part of the experiment was obtaining data on the coefficient of friction, μ, between the robot and the surface. The methods of conducting the experiment were outlined in section III A 2).

Each material went through 25 measurement trials to ensure repeatability and confidence in the results. In each trial, the angle of the surface was slowly increased until the robot began to slip. Once the robot would slide continuously, it the current angle was taken as the slip angle and the surface was then lowered by a couple of degrees and the test was repeated. The slip angle was determined using a protractor application on a smartphone which makes use of the phones internal accelerometer. Mounting the phone was accomplished using a 3D printed stand that was taped to the testing surface in order to prevent sliding. From these tests, friction values for

glass, MDF, brick, and concrete were obtained. The results are summarized below in Table 13.

Trial	Glass	MDF	Brick	Concrete
1	24.8	31.8	32.0	46.2
2	24.0	29.7	30.8	47.0
3	23.5	29.5	30.2	46.5
4	23.0	30.4	30.3	47.5
5	23.4	29.8	32.2	45.7
6	22.8	29.6	30.5	49.0
7	22.6	29.4	30.2	43.0
8	22.7	29.2	30.4	49.5
9	23.0	28.7	30.3	47.2
10	22.7	30.4	29.8	45.0
11	22.9	29.0	31.1	47.7
12	22.6	28.4	30.5	46.6
13	22.6	29.1	30.4	44.8
14	22.4	28.5	30.1	44.5
15	23.6	28.7	33.0	43.8
16	20.6	29.0	32.5	45.5
17	21.4	28.8	30.5	43.8
18	22.4	29.2	31.2	44.3
19	23.6	30.3	33.5	48.0
20	23.8	28.6	30.4	45.5
21	23.0	28.5	31.9	43.6
22	23.3	28.7	31.4	44.8
23	24.1	28.6	31.7	48.9
24	23.6	28.8	32.2	45.2
25	25.1	27.8	31.1	44.6
Average	**23.1**	**29.2**	**31.1**	**45.9**
Standard Dev	**0.95**	**0.85**	**1.00**	**1.81**
μ	**0.43**	**0.56**	**0.60**	**1.03**

Table 13: Slip Angles [Deg] and Calculated Values of μ

Once values for the coefficient of friction of each surface were obtained, theoretical calculations about the robot's performance could be evaluated. This was

accomplished by setting select surfaces to specific values and lowering the thrust of the fan slowly at a given thruster angle and observing when the robot would start to slip. The theoretical equations to determine the static holding force were derived in section I B.

In order to know the actual force exerted by the fan separate experiments were run to measure the thrust force. The set-up of these thrust tests were described in section III A. Two methods were tested and compared to ensure accuracy, the first of which used a strain gauge that was adhered to an aluminum cantilever beam and the second of which used a commercial off the shelf digital cooking scale. Before data was collected with the strain gauge it first needed to be calibrated. Calibration was done by placing lead fishing weights in a 3D printed cup that was placed over the back of the motor on the ducted fan. A picture of this set-up is shown below in Figure 14.

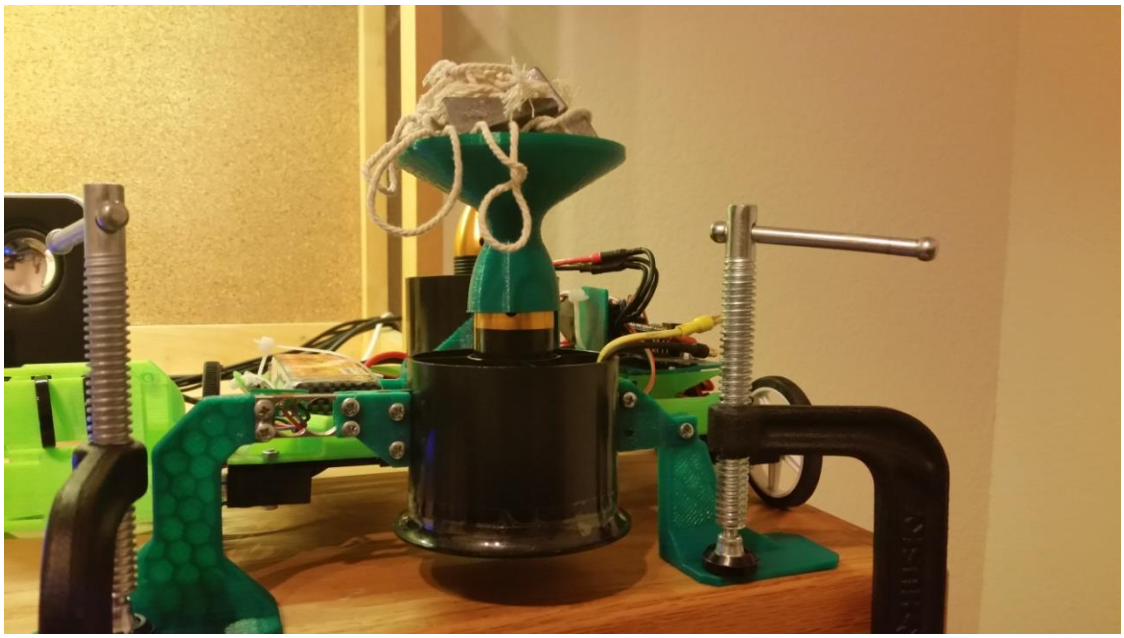

Figure 14: Strain Gauge Calibration Set-up

As weights were placed on the cup, voltage measurements were collected using an Arduino Uno and displayed on a serial terminal every half second. The actual values of the weights were measured using a digital scale beforehand. The results of the measurement and calibration are shown in tabular form in Table 14 as well as a chart in Figure 15.

Weight Added	Gauge Reading
0 g	209 mV
21 g	211 mV
77 g	217 mV
133 g	223 mV
189 g	227 mV
245 g	234 mV
301 g	240 mV
357 g	247 mV
413 g	252 mV
469 g	258 mV

Table 14: Strain Gauge Calibration Table

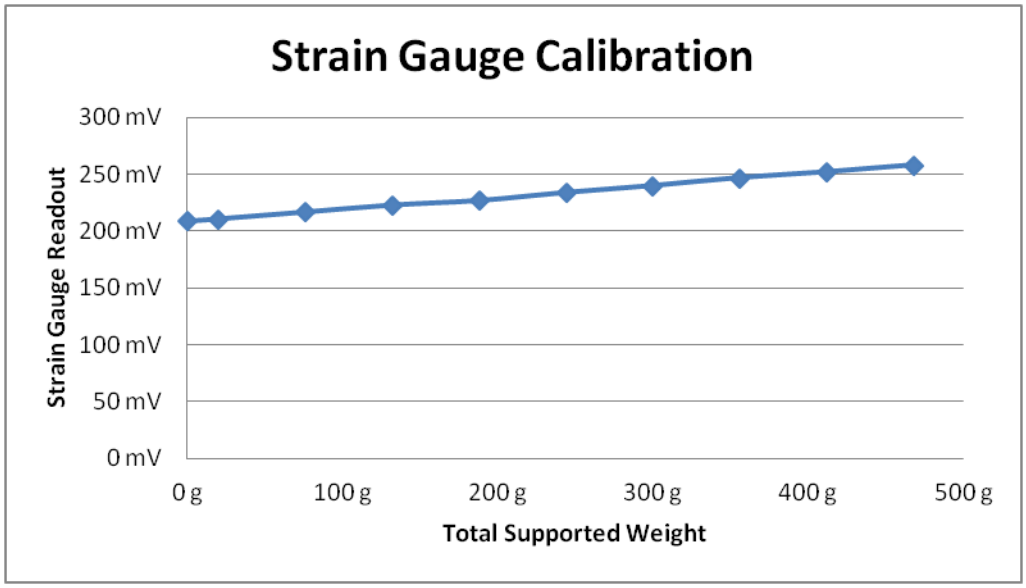

Figure 15: Strain Gauge Calibration Voltage Reading vs Weight

Once calibrated, the strain gauge set-up could then be used to record the actual force values for given thrust settings by the controller. Thrust settings were increased in 10% increments starting at 20% for two different battery types, 11.1V Li-Po and a 14.8V Li-Po. For further verification, results were also obtained using the digital scale

for the same settings, the results of which are tabulated below in Table 15 and Table 16.

11.1V Battery	20%	30%	40%	50%	60%	70%
Average Thrust	2.08 N	4.05 N	5.31 N	7.58 N	7.59 N	7.21 N

Table 15: Digital Scale Measurements for Thrust (11.1V)

14.8V Battery	20%	30%	40%
Average Thrust	3.32 N	5.35 N	7.30 N

Table 16: Digital Scale Measurements for Thrust (14.8V)

A comparison of the two methods is shown in Figure 16 below.

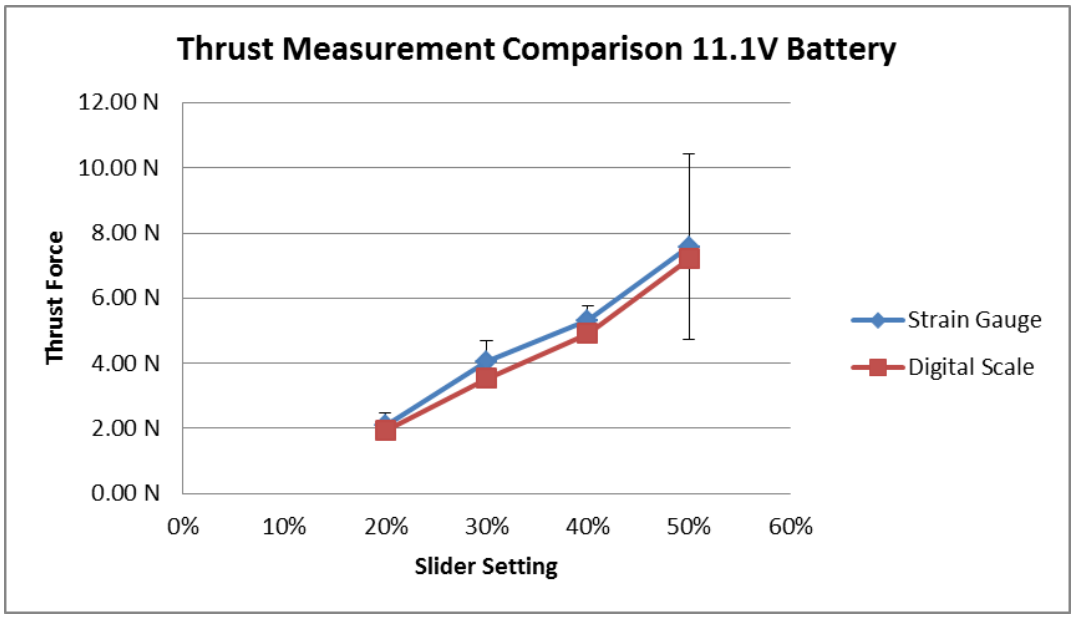

Figure 16: Force Test Comparison

In the strain gauge measurements, ramp up and ramp down periods were excluded and only values where the motor was at full speed were used. In order to eliminate noise, some digital filtering and smoothing was used. Additionally, the battery was fully charged at the beginning of each type of test. From the results it can be seen that there is a fairly linear increase in force output based on slider setting. In the app that controls the robot, the slider setting is really responsible for the duty cycle that is the input for the electronic speed controller.

With actual force values obtained, physical tests could then be compared to theoretical predictions. Using the set-up outlined in section III A, experiments were run on glass and concrete surfaces in order to show clear differences in performance. Theoretical values of thrust needed to keep the robot stationary were calculated and then compared to actual measured values. The results of this can be seen in Table 17.

Material	Wall Angle	Thrust Angle	Theoretical Force	Actual Force
Glass	150	20	134 g	149 g
		30	115 g	132 g
		40	103 g	114 g
	130	20	515 g	536 g
		30	440 g	466 g
		40	395 g	413 g
Concrete	130	20	62 g	114 g
		30	59 g	96 g
		40	57 g	96 g
	110	20	352 g	466 g
		30	331 g	430 g
		40	322 g	395 g

Table 17: Table of Theoretical vs Actual Results

These were then plotted for easier comparison. These can be seen in Figure 17 and Figure 18.

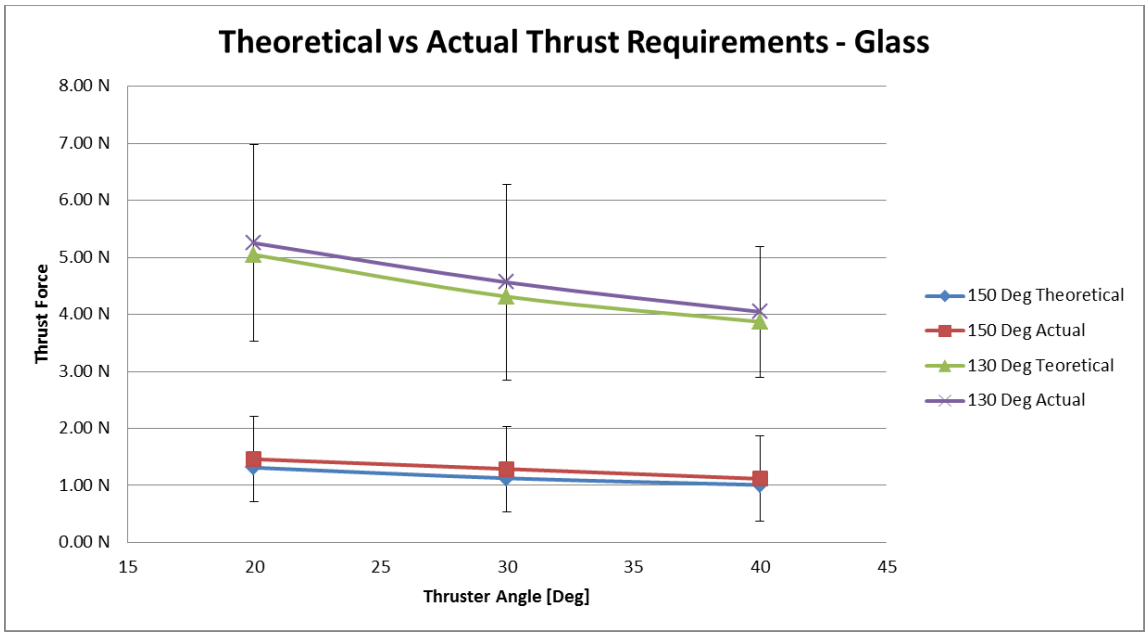

Figure 17: Theoretical vs Actual Performance Characteristics – Glass

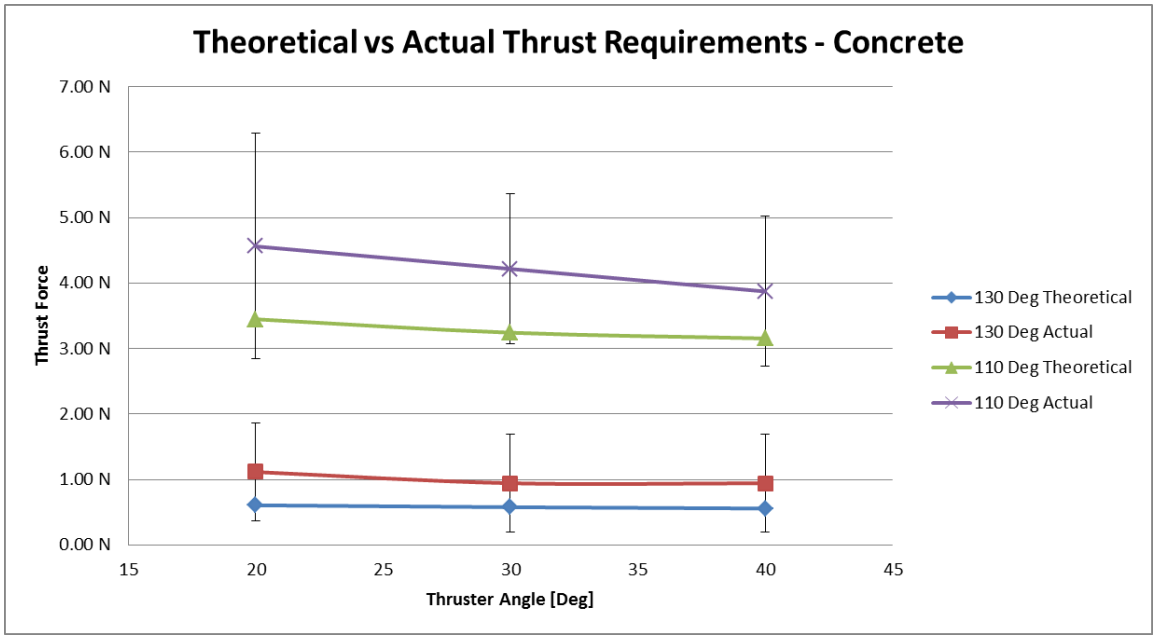

Figure 18: Theoretical vs Actual Performance Characteristics – Concrete

While the actual thrust values needed did vary from the theoretically required values, the trends predicted by the theoretical equations were evident in the actual behavior of the robot.

IV B Results: Experiment 1

Results from this experiment show two different things. The first is simply that this alternate configuration for pneumatic based adhesion could indeed be used to climb on a surface. Secondly it was desirable to show that the robot could climb on surfaces with low coefficients of friction, specifically, lower than 0.74. This number was chosen based on data from Russ Engineering [26] where the average coefficient of friction between rubber and wet concrete was found to be 0.74. By climbing on surfaces with

lower measurements for friction it shows that the robot is able to climb on a wide variety of surfaces as well as wet concrete. From the assumptions in section I D, even though the robot can climb on slick surfaces, it is not designed to be used in the rain.

Tests were run with the robot starting flat on a level surface then transitioning itself into a climbing mode. Since the code used allows the motor to slowly ramp up to full speed, the timer was started after the fan's max speed had been reached at which point the robot would simultaneously start its climb. This was accomplished simply by signaling the robot to move forward at the same time as starting the timer on a tablet app. Twenty-Five trials were conducted for each type of material and measurements were taken for time of climb while parameters for thrust power and thrust angle were chosen. For each type of material it was attempted to choose values that would just start to allow the robot to climb with a little margin of safety. These values are not the absolute limits because as the batteries would drain, the power output would change. Therefore as batteries ran down and needed to be recharged, it was marked when the new battery was installed.

Below, a table for the average thrust output and thrust angle that were used is shown in Table 18.

	Glass	MDF	Brick	Concrete
μ	0.43	0.56	0.6	1.03
Avg. Climb Time	4.38 s	4.52 s	5.05 s	4.16 s
St. Dev	0.73 s	0.63 s	1.10 s	1.35 s
Absolute Force	7.36 N	6.90 N	7.20 N	6.96 N
X Force	4.50 N	3.49 N	4.48 N	4.07 N
Y Force	5.82 N	5.95 N	5.64 N	5.65 N
St. Dev	0.34 N	0.25 N	0.17 N	0.25 N

Table 18: Experiment 1 Results for Thrust Forces Required and Climb Times

While most of the variability was a result of synchronizing the timer to the robot motion, the rougher surfaces experienced a higher rate of variability due to the unevenness of the terrain. This effect was exasperated by the fact that low level values were chosen for thrust output and thrust angle. Higher values resulted in better climbing ability and lowered the likelihood that the robot could get stuck.

For this experiment the thrust output was kept relatively constant and the thrust angle was lowered until the robot was just able to climb with some margin. As expected, the thrust angle required to maintain adhesion dropped as the coefficient of friction between the robot and the surface increased.

IV C Results: Experiment 2

The results from this experiment show the robot's ability to overcome step-like obstacles while climbing. This is important because robots that use suction for adhesion must use a compliant drive system that can deform over the obstacle or risk having the robot loose adhesion and fall. Of robots surveyed, no single body robot could overcome a step obstacle of greater that 10mm in height.

This experiment was broken up into three segments based on obstacle height. The first set-up was for a 5mm obstacle, then a 10mm obstacle, and finally a 15mm obstacle. For each obstacle set-up, twenty-five trials were taken to record the climbing time as well as the thrust output selected and the thrust angle. All trials were run using a 14.8V battery and in all cases, the robot was able to overcome the obstacle while carrying its own power source.

Once again as in experiment 1, near limiting values were chosen for each run in the experiment. This helped to save battery life as well as to give a relative base-line of the settings needed to overcome the given obstacles.

h	5 mm	10 mm	15 mm
Avg. Climb Time	5.84 s	4.83 s	4.56 s
St. Dev	0.57 s	0.34 s	0.25 s
Absolute Force	7.13 N	7.74 N	8.35 N
X Force	4.95 N	5.51 N	6.21 N
Y Force	5.13 N	5.43 N	5.59 N
St. Dev	0.33 N	0.50 N	0.17 N

Table 19: Experiment 2 Results for Thrust Forces Required and Climb Times

From Table 19 it can be seen that as the obstacle height increases, so does the power and thrust angle needed to overcome it. This result is not surprising since as the obstacles get taller, the point of contact on the wheel likewise gets higher and as it does, the wheels act more like they would in transitioning between surfaces. However in each case, the front wheels had little to no trouble driving over the step and all the difficulties where exhibited in the rear wheels. This may merit further study in its own.

IV D Results: Experiment 3

This experiment served to explore the surface transitioning ability of the climbing robot. While other robots exhibit the ability to move from one surface to the other, this is a challenging task for robots that use wheeled motion. In order to accomplish this most robots use multiple bodies with an actuating arm in between. Adding more

bodies increases cost and weight which is then made worse by adding the weight of the mechanism needed to lift the other body.

In addition to the extra weight, more time is needed to ensure adhesion while making the transition. Typically the first body will turn off the active adhesion mechanism, then the connecting arm will actuate, lifting the first body onto the new surface, adhesion from the first body will be resumed, adhesion for the second body will be stopped, the arm will place the new body into position, and finally adhesion will be resumed. By using thrust force, no adhesion is lost during the sharp surface transition and therefore the transition can happen in a passive manner.

This experiment tested this ability using glass and concrete as its surface material because they were at opposite ends of the measured friction range. Table 20 shows the summarized results of the concrete testing.

Concrete	**150-150**		**130-130**		**110-110**		**90-90**		**80**
Absolute Force	0.00 N	3.63 N	2.84 N	7.68 N	8.47 N	8.47 N	7.73 N*	7.73 N*	7.41 N
X Force	0.00 N	1.53 N	1.42 N	5.36 N	4.98 N	4.98 N	2.04 N*	0.75 N*	3.13 N
Y Force	0.00 N	3.29 N	2.46 N	5.51 N	6.85 N	6.85 N	7.46 N*	7.70 N*	6.72 N
standard dev	0.00 N	0.26 N	0.37 N	0.65 N	0.56 N	0.55 N	0.55 N*	0.55 N*	0.00 N

Table 20: Concrete Surface Transition results

Table 21 shows the transition results for glass.

Glass	150-150		130-130		110-110		90-90		80
Absolute Force	3.94 N	3.94 N	6.40 N	8.30 N	6.91 N	7.62 N	6.91 N*	6.91 N*	7.49 N*
X Force	1.91 N	1.91 N	4.83 N	6.26 N	5.22 N	4.68 N	4.44 N*	0.00 N*	5.65 N*
Y Force	3.45 N	3.45 N	4.20 N	5.45 N	4.53 N	6.01 N	5.29 N*	6.91 N*	4.91 N*
standard dev	0.24 N	0.24 N	0.29 N	0.00 N	0.29 N	0.36 N	0.00 N*	0.00 N*	0.34 N*

Table 21: Glass Surface Transition results

There are a few interesting remarks from this experiment. Firstly, any result marked with [*]. Secondly, as angles became more acute, more thruster actuation was needed for the robot to be stable. In many cases this was not easily done by the operator and required lots of time which drew down the battery and would change the force delivered. In the case of a 90-90 degree glass surface, changes in thruster angle were extreme enough that only a few tests could be run and a few times the robot fell and even flew of the test rig. Since damage to the robot was likely as a result of the test, only five trials were run.

From the data above it can be seen that as surfaces became steeper, the amount of fan force needed would increase. This trend is in agreement with the results posted in the preliminary experiments in section IV A. It is interesting to note, however, that fan forces and angles were generally higher in this experiment than they were in the preliminary experiments for the same material and surface angles. This is due, in general, to the need to transition between surfaces instead of simply just adhering to

them. This need is amplified as the angles between surfaces become more drastic since extra force is required to start the transition.

IV E Results: Experiment 4

The focus for this experiment was climbing over a gap of known dimensions. This type of test was important because it is a similar test used in USAR type environments and can present a major obstacle in a robot's ability to main adhesion if using a pneumatic based system. Many different suction based robots are able to climb on surfaces with surface cracks and even brick by utilizing a flexible skirt around the suction area that helps keep the internal pressure low. However, if the gap were to be sufficiently large enough, the robot could possibly lose adhesion and fall. With this configuration, loss of adhesion ceases to be the issue and the only limiting parameter becomes the robot's geometry.

The surface material of choice in this experiment was concrete since it has been the main focus of this research. For each test, two sections of concrete were placed at know distances apart with a known gap depth and the robot attempted to pass over the gap. In this experiment the gap length never exceeded the wheel diameter since this would cause the robot to fall completely into the gap. That kind of scenario could eventually become a separate test in later research.

Gap in Concrete (23mm Depth)				
Gap Length	55mm	45mm	35mm	25mm
Absolute Force	7.71 N*	8.11 N	7.71 N	7.31 N
X Force	5.73 N*	6.02 N	5.73 N	5.43 N
Y Force	5.16 N*	5.42 N	5.16 N	4.89 N
standard dev	0.23 N*	0.33 N	0.32 N	0.26 N

Table 22: Results for Overcoming a Gap-Type Obstacle

From Table 22 it can be seen that for each test the thruster angle remained constant and the parameter that was chosen to change was the thrust power setting. For the most part it was desirable to try to maintain battery life as much as possible and so climbing ability was first increased by increasing the thruster angle as it required no greater amount of battery power. In general as gap length increased, the thrust power needed also increased. This is due the amount that the wheel would fall into the gap and as it dropped deeper in, the robot needed more force to pull or push itself out. These tests were conducted using a 14.8V battery and in all cases except for the 55mm gap case, the robot was able to carry its own power supply.

There was an interesting result for this test in that once again, the back wheel would tend to have the most problems in escaping from the trench. It was thought that since when the front wheels drop, the effective angle of the thruster is lowered, and it is more difficult for the robot to climb but when the back wheels dropped in the trench

the effective angle of the thrust should increase making it easier to climb. While the effective angle did change as predicted it was still more difficult for the back wheels to escape the trench than it was for the front wheels. This is an interesting result that could be investigated further. Possible solutions include using treaded wheels to avoid having specific parts to get stuck. This is an example of a problem area that can hinder the usefulness of climbing robots in real-world scenarios.

V CONCLUSIONS

V A Experiment 1

From the first tests it was shown that the robot was able to climb on surfaces with coefficients of friction as low as 0.43 between the robot and the climbing surface. As expected, the fan force and thrust angle needed increased as the friction of the climbing surface decreased. It is also worth noting that, in general, as the fan force increased the adhesion would increase and therefore the climbing time would be a little lower. However there was enough inconsistency in starting and stopping the timers that any benefit in speed was small compared to human reaction time. This means that for the most part, the range in which the robot would slip a lot but still climb (leading to slow climb times) is very small. The results are more binary in that it would either climb at a predictable speed or not at all.

Showing that the robot can climb on a smooth or a slick surface is important because many times as the surface becomes slicker, it is more difficult to maintain adhesion. By climbing on slick surfaces the robot is demonstrating that it has the ability to tackle a wide variety of surfaces with different coefficients of friction. Assuming a flat surface geometry where only the friction could vary, higher coefficients of friction only make climbing easier for the robot. It is then desirable to climb on the surface with the lowest coefficient of friction possible. The other side of that problem is to

naturally let the robot have a high coefficient of friction between itself and surfaces, making adhesion easier.

The goal of this test was to show that the robot could climb on a variety of surfaces even when coefficients of friction dropped low. By testing four different surfaces that are found in industrial building materials, the robot has shown that it could climb on any flat, vertical surface where those materials are used.

V B Experiment 2

The second experiment set out to show that the robot could overcome obstacles while climbing vertically. It showed that, for a single body robot that is wheel driven, the robot could overcome a step obstacle that was taller than any of the other robots that were surveyed could overcome. The maximum step height that was surveyed was found to be 10mm and was accomplished by the robot City Climber [39]. Experiment 2 showed that the robot CR4 was able to climb over a step with a height of 15mm. While it was able to accomplish this it required lots of power as the step height increased. Additionally it was very easy for the back wheels to get stuck which suggests that greater normal force on the back wheels may be necessary.

It could be seen that the climbing time generally decreased based on the obstacle height, a counter intuitive result. This is likely a result of the fact that more force was required for the higher step height and therefore the robot would grip slightly better.

Additionally since the angle of the fan was higher, it contributed to greater assistance while climbing.

V C Experiment 3

Transitioning between surfaces was both a desirable climbing robot ability as well as an application of a USAR type test. In a USAR type test a robot is usually required to be able to move up an inclined plane. Without any assistance from an adhesion system, there is a maximum angle that the robot can climb without slipping. While it may be possible to simply increase the weight of a ground based robot, this would be generally undesirable for many other reasons. Instead by adding thrusters, greater normal force can be achieved only when needed and be used to possibly climb vertically as this research suggests.

As expected, steeper angles required more thrust force and a greater thrust angle. Although, as the robot entered into inverted climbing, the thrust angle needed to be lowered again. In the case where the robot was completely inverted, the thrust angle needed to be normal to the surface for maximum holding force. Some set-ups such as the 80-80 degree inclines were technically possible but took lots of time due to the wide range of thrust angles needed. This type of environment would be greatly aided by letting the fan angle be passively controlled. In this way the operator simply has to control the direction of the robot and the microcontroller can set the angle of the thruster to best maintain adhesion. Since this method was not in place at the time of

testing, more extreme angles were not tested in order to protect the robot. This was also the case for the 70 degree inverted angle.

For many of the surface angles tested using an 11.1V battery was enough to accomplish the climbing goals but for more aggressive angles the 14.8V battery was needed. Carrying the extra weight of the larger 14.8V battery may be undesirable in some cases, especially if it is know that the robot would only encounter shallow angles. In other cases the weight of the battery was too much and it needed to be removed and the robot run under tethered operation. This issue will be discussed more in the Future Work section.

V D Experiment 4

The last experiment was another USAR type of experiment. While in USAR type tests the trenches may be quite far across, this is harder in the case of climbing robots because adhesion must be maintained during the crossing. By conducting this test it is meant to start a new standard in climbing robot abilities.

While the robot exhibited the expected trend with respect to needing more thrust force and thrust angle as the gap length increased, it was interesting to see that once again the rear wheels had the most difficulty in overcoming the obstacle. Additionally it was found that there was indeed a limit below 55mm where the robot could not cross and carry its own power source. The largest tested successful gap length was

45mm while untethered; crossing a 55mm gap was only possible under tethered operation. There are possible solutions to this problem but they will be discussed in the Future Work section.

V E Future Work

Letting the thruster on the robot be passively controlled by the microcontroller will make the robot more user friendly and increase its battery life by allowing for faster surface transitions. This could be accomplished by adding an accelerometer to the body of the robot that would constantly measure the robots orientation to a vertical surface. It would be highly recommended to make a vertical wall be 0 degrees and measurements be taken about that point of origin. A small mount would probably need to be modeled and printed, then screwed into the robot chassis. The base code would then need to be edited to read the angle of the robot body and adjust the fan accordingly. Inputs about the friction coefficient of the surface are needed. Use the experiments of this thesis as a baseline for required outputs and allow some safety margin.

A user enabled “Grip Mode” would require changing the app and adding the button and the character message to be sent through Bluetooth. This mode, when toggled, would increase the fan force by some small amount and lower the drive speed. This would be used in cases where the robot might be adhering to the surface but is slipping. Lowering the drive speed should lower the torque exerted on the motor and

the increased fan speed should increase the normal force on the wheels, giving it a better grip on the surface. Since this might draw a lot more power, it should only be used as needed.

Some protection is needed at the inlet side of the fans. When driving outside it is possible for leaves, twigs, and small rocks to get sucked into the fan and thrown out the other side. This poses a potential danger to the user as well as possibly resulting in catastrophic failure of the robot. When designing the inlet protection it is still important to allow sufficient airflow through the fans.

Currently the app uses arrow buttons to control the direction of the robot. Based on the way the code is written, two buttons cannot be pressed simultaneously. Instead of buttons to control the direction a touch pad section, like in many app games, might be more efficient. Change the app to add in this section and let the program readout the x and y coordinates with 0 set in the middle. Send the coordinates through to the Arduino and compute the magnitude and direction. Adjust the wheel speeds based on these results to give better handling.

The current design uses two batteries. A small one that is responsible for driving the wheels, and a larger one that powers the fans. If a custom power distribution board was designed it could eliminate the need for the smaller battery as well as some of the wiring. Using electrical CAD software such as KiCAD or EagleCAD, a new board can be designed with the necessary components to provide 11.1V from the battery to the

fans and 9V to the DC motor drivers. Each of the motor drivers used can provide 5V to the microcontroller so nothing else is needed. This would then need to be mounted onto the chassis.

Upgrade the wheels to treads, this will increase the gripping ability of the robot and therefore require less fan force. Additionally treads would make it easier by far to overcome obstacles. They will need to be custom made in order to be effective since store bought treads are typically made out of plastic or hard rubber and will not offer the same gripping power as a two part silicone mix. The wheels will need to be replaced with custom designed wheels that interlock with the treads.

Shock absorbers would greatly benefit the robot in its abilities to overcome obstacles. Once RC shock absorbers are purchased, a mounting system must be designed and printed, or laser cut, that allows the wheels to move compliantly without letting the tread slip off. Keep the wheels in line with each other. Lots of work will need to be done to add this feature without adding a lot of weight.

The use of multiple bodies may also help the overall performance of the robot by consolidating functions and giving more holding ability. As more modules are added, the overall robot will have greater and greater excess thrust capacity that can be used to lift heavier objects. In addition, more modules will help pull or push module sections over obstacles and increase the robot's overall robustness.

V F Final Robot Specifications

Final Specs for CR4.3	
Robot Weight	8.20 N
Maximum Thrust	9.30 N
Maximum Thrust Angle	48°
Maximum Climbing Speed Tested	8.32 m/s
Communication	Bluetooth
Locomotion Method	Wheeled
Adhesion Method	Thrust
Thruster Battery	14.8V, 2200 mAh
Drive Battery	7.4V, 1000 mAh

WORKS CITED

[1] J. T. Machado and M. F. Silva, "A Survey of Technologies and Applications for Climbing Robots Locomotion and Adhesion," Porto, Portugal.

[2] T. P. Sattar, H. L. Rodriguez and B. Bridge, "Climbing Ring Robot for Inspection of Offshore Wind Turbines," *Industrial Robot,* pp. 326-330, 2009.

[3] G. C. Haynes, A. Khripin, G. Lynch, J. Amory, A. Saunders, A. A. Rizzi and D. E. Koditschek, "Rapid Pole Climbing with a Quadrupedal Robot," International Conference on Robotics and Automation, Kobe, Japan, 2009.

[4] M. F. Silva and J. T. Machado, "New Technologies for Climbing Robots; Adhesion Surfaces," Porto, Portugal.

[5] K. Schlee and B. Schlee, "Mobile Robot". United States Patent 13/690,951, 30 November 2012.

[6] B. Kennedy, A. Okon, H. Aghazarian, M. Badescu, X. Bao, Y. Bar-Cohen, Z. Chang, B. E. Dabiri, M. Garrett, L. Magnone and S. Sherrit, "Lemur IIb: A Robotic System for Steep Terrain Access," JPL, Pasadena, California, 2005.

[7] S. Fujii, K. Inoue, T. Takubo and T. Arai, "Climbing up onto Steps for Limb Mechanism Robot “ASTERISK”," Graduate School of Engineering Science Osaka University, Osaka, Japan, 2006.

[8] T. Kang, H. Kim, T. Son and H. Choi, "Design of Quadruped Walking and Climbing Robot," in *Intl. Conference on Intelligent Robots and Systems*, Las Vegas, Nevada, 2003.

[9] D. Schmidt and K. Berns, "Climbing Robots for Maintenance and Inspections of Vertical Structures—A Survey of Design Aspects and Technologies," *Robotics and Autonomous Systems,* vol. 61, pp. 1288-1305, 2013.

[10] H. Zhu, Y. Guan, C. Cai, L. Jiang, X. Zhang and H. Zhang, "W-Climbot: A Modular Biped Wall-Climbing Robot," in *International Conference on Mechatronics and Automation*, Xi'an, China, 2010.

[11] J. Yu, S. Chary, S. Das, J. Tamelier, N. Pesika, K. Turner and J. Isrealachvili, "Gecko-Inspired Dry Adhesive For Robotic Applications," *Materials Views,* pp. 3010-3018, 2011.

[12] Z. Burton, "Surface Characterization, Adhesion, and Friction Properties of Hydrophobic Leaf Structures and Nanopatterned Polymers for Superhydrophobic Surfaces," Ohio, 2005.

[13] M. Murphy, C. Kute, Y. Menguc and M. Sitti, *International Journal of Robotics Research,* pp. 118-133, 2011.

[14] M. Murphy, B. Aksak and M. Sitti, "Adhesion and Anisotropic Friction Enhancements of Angled Heterogeneous Micro-Fiber Arrays with Spherical and Spatula Tips," *Journal of Adhesion Science and Technology,* vol. 21, no. 12-13, pp. 1281-1296, 2013.

[15] B. Aksak, M. P. Murphy and M. Sitti, "Gecko Inspired Micro-Fibrillar Adhesives for Wall Climbing Robots on Micro/Nanoscale Rough Surfaces," in *IEEE International Conference on Robotics and Automation*, Pasadena, CA, 2008.

[16] I. M. Koo, D. T. Trong, Y. H. Lee, H. Moon, J. Koo, S. K. Park and H. R. Choi, "Development of Wall Climbing Robot System by Using Impeller Type Adhesion Mechanism," *J Intell Robot Syst,* vol. 72, p. 57–72, 2013.

[17] S. D. Francisci, D. Longo and G. Muscato, "A Direction Dependent Parametric Model for the Vacuum Adhesion System of the Alicia II Robot," IEEE, Catania, Italy, 2006.

[18] D. Schmidt, "Safe Navigation of a Wall-Climbing Robot - Risk Assessment and Control Methods," Technischen Universität Kaiserslautern, Germany, 2013.

[19] J. Xiao, W. Morris, N. Chakravarthy and A. Calle, "City-climber: a New Generation of Mobile Robot with Wall-climbing," *SPIE,* vol. 6230, 2006.

[20] G. Lee, G. Wu, S. H. Kim, J. Kim and T. W. Seo, "Combot: Compliant Climbing Robotic Platform with Transitioning Capability and Payload Capacity," in *IEEE International Conference on Robotics and Automation* , Saint Paul, Minnesota, USA , 2012.

[21] T. W. Seo and M. Sitti, "Under-Actuated Tank-Like Climbing Robot With Various Transitioning Capabilities," in *IEEE International Conference on Robotics and*

Automation, Shanghai, China, 2011.

[22] J. Liu, S. Ma, Z. Lu, Y. Wang, B. Li and J. Wang, "Design and Experiment of a Novel Link-Type Shape Shifting Modular Robot Series," in *IEEE International Conference on Robotics and Biomimetics*, Shatin, 2005.

[23] C. Ye, S. Ma and B. Li, "Design and Basic Experiments of a Shape-shifting Mobile Robot for Urban Search and Rescue," in *International Conference on Intelligent Robots and Systems*, Beijing, China, 2006.

[24] S. Tadokoro, "Rescue Robotics Challenge," IEEE, Seoul, 2010.

[25] R. A. Serway and R. J. Beichner, Physics for Scientists and Engineers with Modern Physics 5th edition, New York: Saunders.

[26] I. Russ Engineering Group, "Results of Friction Coefficient Test," Russ Engineering Group, Inc., Baton Rouge, La., 2000.

[27] Y. M. El-Sherbiny, A. T. Hasouna and W. Y. Ali, "Friction Coefficient of Rubber Sliding Against Flooring Materials," *ARPN Journal of Engineering and Applied Sciences,* vol. 7, no. 1, pp. 121-126, 2012.

[28] B. Persson, "Rubber Friction: Role of the Flash Temperature," *Journal of Physics: Condensed Matter,* vol. 18, no. 32, pp. 7789-7823, 2006.

[29] D. Quick, "Student Runs Crawl Concept Up Ulility Pole For James Dyson Awards," gizmag, 8 October 2012. [Online]. Available: http://www.gizmag.com/crawl-dyson-awards/24456/. [Accessed 13 May 2015].

[30] Mitutoyo, "Practical tips for laboratory and workshop," in *Surface Roughness Measurement*, Aurora, Illinois, Mitutoyo America Corporation, 1984.

[31] P. M. Santos and E. N. Julio, "Comparison of Methods for Texture Assessment of Concrete Surfaces," *ACI Materials Journal,* vol. 107, no. 5, pp. 433-440, 2009.

[32] M. D'Orazio, G. Cursio, L. Graziani, L. Aquilanti, A. Osimani, F. Clementi, C. Yepremain, V. Lariccia and S. Amoroso, "Effects of Water Absorption and Surface Roughness on the Bioreceptivity of ETICS Compared to Clay Bricks," *Building and Environment,* vol. 77, pp. 20-28, 2014.

[33] O. Unver, A. Uneri, A. Aydemir and M. Sitti, "Geckobot: A Gecko Inspired Climbing Robot Using Elastomer Adhesives," in *IEEE International Conference on Robotics and Automation*, Orlando, Florida, 2006.

[34] G. Peters, D. Pagano, K. Liu and K. Waldron, "A Prototype Climbing Robot for Inspection of Complex Ferrous Structures," in *International Conference on Climbing and Walking Robots*, Nagoya, Japan, 2010.

[35] Y. Zhao, T. Tong, L. Delzeit, A. Kashani, M. Mayyappan and A. Majumdar, *Vacuum Sci. Technol.,* vol. 24, pp. 331-335, 2006.

[36] C. Menon and M. Sitti, "Biologically Inspired Adhesion Based Surface Climbing Robots," in *International Conference on Robotics and Automation*, Barcelona, Spain, 2005.

[37] S. Aravind, M. Amritha, R. Sanju, R. Akhil, S. Vijitha and B. Gauri, "A Novel Design Technique to Develop a Low Cost and Highly Stable Wall Climbign Robot," in *International Conference on Intelligent Systems, Modelling and Simulation*, Bangkok, 2013.

[38] Y. Yoshida and M. Shugen, "Design Of A Wall Climbing Robot With Passive Suction Cups," in *International Conference on Robotics and Biomimetics*, Tianjin, 2010.

[39] J. Xiao, A. Sadegh, M. Elliott, A. Calle, A. Persad and H. M. Chiu, "Design of Mobile Robots with Wall Climbing Capability," in *International Conference on Advanced Intelligent Mechatronics*, Monterey, California, 2005.

[40] A. Leibbrandt, G. Caprari, U. Angst, R. Y. Siegwart, R. J. Flatt and B. Elsener, "Climbing Robot for Corrosion Monitoring of Reinforced Concrete Structures," in *International Conference on Applied Robotics for the Power Industry*, ETH Zurich, Switzerland., 2012.

[41] J. Troy, S. Lea, E. Georgeson, K. Nelson and C. Richards, "Holonomic Motion Vehicle for Travel on Non-Level Surfaces". USA Patent US 8,738,226 B2, 27 May 2014.

[42] J.-U. Shin, D. Kim, J.-H. Kim and H. Myung, "Micro aerial vehicle type wall-climbing robot mechanism," in *IEEE International Symposium on Robot and Human Interactive Communication*, Gyeongju, Korea, 2013.

[43] S. Hirose, A. Nagakubo and R. Toyama, "A Machine That Can Walk and Climb on Floors, Walls and Ceilings," IEEE, Tokyo, Japan, 1991.

[44] S. P. Krosuri and M. A. Minor, "A Multifunctional Hybrid Hip Joint for Improved Adaptability in Miniature Climbing Robots," in *International Conference on Robotics & Automation*, Taipei, Taiwan, 2003.

[45] D. A. v. Beek, "Tribology-ABC," Engineering-ABC, 2012. [Online]. Available: http://www.tribology-abc.com/abc/friction.htm. [Accessed 2 10 2014].

[46] E. R. Jones and R. L. Childers, Contemporary College Physics, Addison-Wesley, 1990.

[47] E. L. Nichols and W. S. Franklin, The Elements of Physics: A College Textbook, University of California: Macmillan, 1898.

APPENDIX

A. Code Used

MIT App Inventor 2 Code

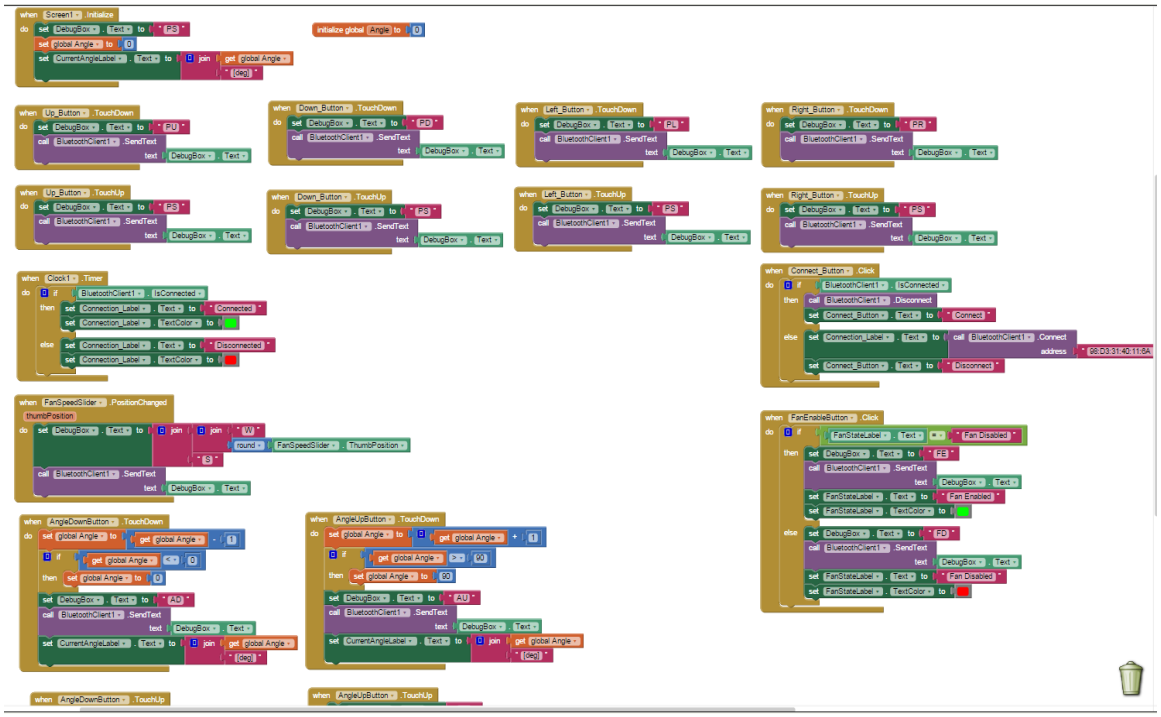

/*

Climbing Robot v4 (CR4)

v3.0

This code enables the robot to listen to commands through a bluetooth connection.

Commands are given as characters through an app running on an andriod platform.

This includes basic functions such as driving, turning, control of the fan and fan speed,

and control of the fan angle.

Written by Alex Stockton

*/

```
//#include <SoftwareSerial.h>

#include <Servo.h>



//SoftwareSerial mySerial(10, 11); // RX, TX



Servo fan;

Servo driveL;

Servo driveR;

Servo thrustServo;
```

```
int MaxFanSpeed;

int CurrFanSpeed;

int RampSpeed;

int DriveSpeed_L;

int DriveSpeed_R;

int ThrustAngle;

int fan_accel = 10; //[%/sec]

int accel_time = 1/fan_accel*1000; //[ms]

int comm_delay = 20;

const int powerpin = 2;

const int offset = 7;



String MotorSpeedChar;

String FanSpeedChar;

String ThrustAngleChar;

char dir;
```

```
boolean FanState;



void setup()

{

  // Open serial communications and wait for port to open:

  Serial.begin(9600);

  //while (!Serial) {

  //  ; // wait for serial port to connect. Needed for Leonardo only

  //}

  pinMode(powerpin, OUTPUT);

  digitalWrite(powerpin, HIGH);



  //Serial.println("Arduino Interface Connected");



  // set the data rate for the SoftwareSerial port
```

```
//mySerial.begin(9600);

//mySerial.begin(115200);

//Serial.println("Bluetooth Interface Connected");



driveL.attach(6);

driveR.attach(9);

//Serial.println("Drive Motors Connected");



thrustServo.attach(5);

//Serial.println("Servo Thruster Connected");

thrustServo.write(0+offset);



FanState = false;

CurrFanSpeed = 0;

fan.attach(3);

fan.write(10);
```

```
  delay(1500);
}

void loop() // run over and over
{
   // read the value
   char ch1 = Serial.read();
   delay(comm_delay);
   // Look out for a newline character
   if (ch1 == 'P'){
     char ch2 = Serial.read();
     delay(comm_delay);
     switch (ch2){
     case 'U':
        //Serial.println("Moving Up");
        dir = 'U';
```

```
    drive(dir);
    break;
case 'D':
    //Serial.println("Moving Down");
    dir = 'D';
    drive(dir);
    break;
case 'L':
    //Serial.println("Turning Left");
    dir = 'L';
    drive(dir);
    break;
case 'R':
    //Serial.println("Turning Right");
    dir = 'R';
    drive(dir);
```

```
    break;
  case 'S':
    //Serial.println("Stop");
    dir = 'S';
    drive(dir);
    break;
  default:
    //Serial.println("Default");
    dir = 'S';
    drive(dir);
  }
}


if(ch1 == 'A'){
  char ch2 = Serial.read();
  delay(comm_delay);
```

```
switch (ch2){
case 'U':
   //Serial.println("Rotating Up");
   ThrustAngle += 1;
   if(ThrustAngle > 90+offset){
     ThrustAngle = 90+offset;
   }
   thrustServo.write(ThrustAngle);
   break;
case 'D':
   //Serial.println("Rotating Down");
   ThrustAngle -= 1;
   if(ThrustAngle < 0+offset){
     ThrustAngle = 0+offset;
   }
   thrustServo.write(ThrustAngle);
```

```
    break;
  case 'S':
    // Do Nothing
    break;
  }
}

if(ch1 == 'W'){
 while (1) {
   char ch2 = Serial.read();
   delay(comm_delay);
   if (ch2 == 'S'){
    break;
   }
   FanSpeedChar += ch2;
  }
```

```
    //Serial.print("Setting Fan Speed to: ");
    //Serial.println(FanSpeedChar);

    // Conver the char to an integer.
    MaxFanSpeed = FanSpeedChar.toInt();
    //Serial.println(MaxFanSpeed);

    FanMode(FanState, MaxFanSpeed, CurrFanSpeed, accel_time);

    // Reset the input values
    FanSpeedChar = "";
}

if(ch1 == 'F'){
 char ch2 = Serial.read();
 delay(comm_delay);
```

```
    if(ch2 == 'E'){
      //Fan Enabled
      FanState = true;
      FanMode(FanState, MaxFanSpeed, CurrFanSpeed, accel_time);
    }
    else{
      //Fan Disabled
      FanState = false;
      FanMode(FanState, MaxFanSpeed, CurrFanSpeed, accel_time);
    }
   }
}


////////////////////////////////////////////////////////////

//////////////////////  FUNCTIONS  ////////////////////////

////////////////////////////////////////////////////////////
```

```
int drive( ){



 //driveR.write(130);

 driveL.write(130);

 driveR.write(110);

 delay(50);



 DriveSpeed_L = 80;

 DriveSpeed_R = 80;



 switch(dir){

  case 'U':

    // Set the drive speed

    DriveSpeed_L = map(DriveSpeed_L, 0, 100, 90, 140);

    DriveSpeed_R = map(DriveSpeed_R, 0, 100, 90, 140);

    break;
```

```
case 'D':
  DriveSpeed_L = map(DriveSpeed_L, 0, 100, 90, 40);
  DriveSpeed_R = map(DriveSpeed_R, 0, 100, 90, 40);
  break;
case 'L':
  DriveSpeed_L = map(DriveSpeed_L, 0, 100, 90, 40);
  DriveSpeed_R = map(DriveSpeed_R, 0, 100, 90, 140);
  break;
case 'R':
  DriveSpeed_L = map(DriveSpeed_L, 0, 100, 90, 140);
  DriveSpeed_R = map(DriveSpeed_R, 0, 100, 90, 40);
  break;
case 'S':
  DriveSpeed_L = 0;
  DriveSpeed_R = 0;
```

```
    DriveSpeed_L = map(DriveSpeed_L, 0, 100, 90, 140);
    DriveSpeed_R = map(DriveSpeed_R, 0, 100, 90, 140);

    break;
  }

  driveL.write( );
  driveR.write( );

}

int FanMode( ){
  if(FanState == true){ //fan is enabled
    for(int i = CurrFanSpeed; i <= MaxFanSpeed; i++){
      RampSpeed = map(i, 0, 100, 50, 180);
      fan.write(RampSpeed);
```

```
      //delay(accel_time);
      delay(100);
      checkStop(FanState);
      CurrFanSpeed = RampSpeed;
    }
  }
  else{
    fan.write(40);
    CurrFanSpeed = 0;
  }
  return CurrFanSpeed;
}

int checkStop(boolean FanState){
  if(FanState == false){
    fan.write(40);
```

```
    CurrFanSpeed = 0;

    return CurrFanSpeed;

  }

}
```

B. Bill of Materials

CR Series BOM

Item	Price	Qnty.	Total	Source
150:1 Micro Metal Gearmotor	$15.95	4	$63.80	Pololu.com
Pololu Wheel 60x8mm (Qty. 2)	$7.95	2	$15.90	Pololu.com
Micro Gearmotor Enclosure	$0.99	4	$3.96	ServoCity.com
3000KV Brushless Motor Ducted Fan 70mm	$27.30	2	$54.60	Amazon.com
SG90 Servo RC Motor (Qty. 5)	$15.99	1	$15.99	Amazon.com
Arduino Nano	$5.00	1	$5.00	Amazon.com
HC-06 Bluetooth Receiver for Arduino	$7.99	1	$7.99	Amazon.com
Skywalker 40A BLDC ESC	$14.48	2	$28.96	Amazon.com
Hobbypower RC 20A ESC Brushed DC Motor	$11.97	2	$23.94	Amazon.com

ADNS 3080 Opical Flow Sensor	$39.99	2	$79.98	3D Robotics.com
Acrylic Chassis	$25.00	1	$25.00	Custom Job
Bluecell 50 PCS RED LED	$2.07	1	$2.07	Amazon.com
Floureon 11.1V 2200mAh LiPo RC Battery	$39.99	1	$39.99	Amazon.com
HobbyKing 7.4V 1000mAh LiPo RC Battery	$12.81	1	$12.81	Amazon.com
M3 Machine Screws 10mm (Qty. 100)	$2.60	1	$2.60	McMaster-Carr.com
M3 Machine Screws 20mm (Qty. 100)	$3.08	1	$3.08	McMaster-Carr.com
M2 Machine Screws 10mm (Qty. 100)	$3.67	1	$3.67	McMaster-Carr.com
M3 Nut (Qty. 100)	$1.39	2	$2.78	McMaster-Carr.com
M2 Nut (Qty. 100)	$1.39	1	$1.39	McMaster-Carr.com
			$393.5	
Total			1	